J Fluoresc (2012) 22:1313–1343
DOI 10.1007/s10895-012-1073-x

ORIGINAL PAPER

Fluorescent Probe Studies of Polarity and Solvation within Room Temperature Ionic Liquids: A Review

Shubha Pandey · Sheila N. Baker · Siddharth Pandey · Gary A. Baker

Received: 15 March 2012 / Accepted: 29 May 2012 / Published online: 19 June 2012

Abstract Ionic liquids display an array of useful and sometimes unconventional, solvent features and have attracted considerable interest in the field of green chemistry for the potential they hold to significantly reduce environmental emissions. Some of these points have a bearing on the chemical reactivity of these systems and have also generated interest in the physical and theoretical aspects of solvation in ionic liquids. This review presents an introduction to the field of ionic liquids, followed by discussion of investigations into the solvation properties of neat ionic liquids or mixed systems including ionic liquids as a major or minor component. The ionic liquid based multicomponent systems discussed are composed of other solvents, other ionic liquids, carbon dioxide, surfactants or surfactant solutions. Although we clearly focus on fluorescence spectroscopy as a tool to illuminate ionic liquid systems, the issues discussed herein are of general relevance to discussions of polarity and solvent effects in ionic liquids. Transient solvation measurements carried out by means of time-resolved fluorescence measurements are particularly powerful for their ability to parameterize the kinetics of the solvation process in ionic liquids and are discussed as well.

Keywords Ionic liquids · Fluorescent probes · Solvatochromic · Polarity · Solvent relaxation

S. Pandey · G. A. Baker (✉)
Department of Chemistry, University of Missouri-Columbia,
Columbia, MO 65211, USA
e-mail: bakergar@missouri.edu

S. N. Baker (✉)
Department of Chemical Engineering,
University of Missouri-Columbia,
Columbia, MO 65211, USA
e-mail: bakershei@missouri.edu

S. Pandey (✉)
Department of Chemistry, Indian Institute of Technology Delhi,
Hauz Khas, New Delhi 110016, India
e-mail: sipandey@chemistry.iitd.ac.in

Introduction

Solvent choice is amongst the most important factors governing the efficiency, rate, selectivity, and outcome of a chemical conversion, extraction, or separation [1, 2]. Recent environmental legislation including the Montreal Protocol, however, has imposed limits on, or even completely banned, the use of several common organic solvents, especially halogenated ones. In an effort to develop and exploit more "environmentally-benign" or "green" solvents and processes, several principal strategies have emerged. While the ultimate goal is, of course, complete elimination of the solvent (heterogeneous catalysis), for many applications performing a reaction "neat" is not possible. More sustainable and friendlier alternatives to hazardous solvents currently in use include aqueous media, compressed or supercritical fluids, fluorous phases and, most recently, *ionic liquids*.

Totally ionic and yet frequently fluid at or below room temperature, ionic liquids represent an exciting departure from ordinary molecular organic solvents with enormous potential in synthesis, non-aqueous biocatalysis, separations, chemical analysis, electrochemistry and electrodeposition, nuclear reprocessing, materials design and process chemistry [3]. Driven by the idea that they offer an "environmentally-responsible" industrial alternative to future reliance on volatile organic compounds (VOCs), ionic liquids have become the subjects of tremendous research effort.

But, what exactly *are* ionic liquids and why have they generated so much excitement?

Simply put, ionic liquids are low-melting salts (some synonyms in the older literature that fit the current working definition of an ionic liquid include "low-", "room-" or "ambient-temperature molten salt", "liquid organic salt", and "ionic fluid"). Of course, what constitutes "low" is decidedly subjective. Gaining broad acceptance, however, is the notion that the term *ionic liquid* be reserved for salts that liquefy at or below 100 °C. Although completely arbitrary (coincident with the boiling point of water), adoption of this definition can be justified by the fact that only salts that are fluid below 100 °C are likely to act as general substitutes for conventional organic solvents in existing processes. And while it may seem aberrant to classify 100 °C as "low temperature" one should consider the characteristically brittle and much higher-melting classical inorganic salts exemplified by common table salt (sodium chloride, NaCl). In such conventional molten salts, which consist of infinite three-dimensional arrays of close-packed spherical ions, strong electrostatic interactions manifest in high lattice energies and melting points of many hundreds of degrees; for example, the melting point for NaCl is near 800 °C. We should point out that although ionic liquids have an upper melting point bound of 100 °C, with few exceptions, those described in this review are in fact molten at room temperature or well below. In practice, such ionic liquids may usually be handled like ordinary, albeit somewhat viscous, solvents. Henceforth, when we use the term *ionic liquid* we connote one that is fluid at room temperature; all else will be referred to as a "molten salt" for the purposes of this review.

The origins of modern day ionic liquid research date to much earlier than one might think given the current attention they enjoy. In fact, interest in this subject extends beyond the last century when molten salt systems piqued the curiosity of Faraday himself [4]. Too, the term *ionic liquid* is a continually evolving one with an eminent prehistory including the field of classical "molten" or "fused" salts just mentioned. These too are fully ionized solvents, however, they differ implicitly in both the melting temperature and the ion motif involved. That is, molten salts consist wholly of inorganic ions and even their eutectic mixtures only rarely melt below 150 °C. For example, the LiCl/KCl eutectic mixture once employed as a salt electrolyte in thermal batteries does not melt until 355 °C. Notable exceptions include the chloroaluminates, mixtures of alkali halides and aluminum chloride; for example, $NaCl/AlCl_3$ has a eutectic composition with a melting point of 107 °C. In ionic liquids, on the other hand, usually one or both ions are polyatomic charge-diffuse organic species with low point group symmetry. As shown in Figure 1, the *typical* ionic liquid is based on a bulky, functionalized and low-symmetry cation paired with a variety of polar and often weakly coordinating anions such as $[(CF_3SO_2)_2N]^-$, henceforth abbreviated $[Tf_2N]^-$. Among those described in the literature, the most widely known are those containing the *N*,*N*′-dialkylimidazolium cation followed by tetraalkylammonium, *N*-alkylpyridinium, *N*,*N*-dialkylpyrrolidinium and tetraalkylphosphonium types.

Although the preparation of ethylammonium nitrate, $[EtNH_3][NO_3]$, a stable organic salt which melts at ca. 12 °C, was described nearly a century ago, inexplicably this breakthrough went virtually unnoticed at the time. It was not until the early 1980s that interest in these salts was revived with evidence by Evans et al. [5] that $[EtNH_3][NO_3]$ supported micelle formation by certain surfactants such as the *N*-alkylpyridinium bromides. By this time, the chloroaluminate ionic liquids were being actively studied by the groups of Osteryoung, Wilkes, Hussey and Seddon [6–8]. The chloroaluminates, direct ancestors of the present day ionic liquid, were, unfortunately, difficult to handle in the laboratory being both extremely reactive toward water and very oxophilic, making them incompatible with common organic solvents including alcohols and acetone. On the other hand, until recently the severely limited variety of organic ionic liquids had relegated them to the realm of mere laboratory curiosity with no practical use envisioned. At present, synthetic routes to several hundred room temperature ionic liquids are known, allowing the preparation of countless others using parallel methods. This dramatic growth can be traced to the development of second-generation ionic liquids that do not require anhydrous handling conditions, a milestone first reported in 1992 by Wilkes and Zaworotko [9]. Their preparation involved anion metathesis between 1-ethyl-3-methylimidazolium iodide, [emim][I], and a number of silver salts, AgX or Ag_2X ($X=NO_2^-$, NO_3^-, BF_4^-, $CH_3CO_2^-$, SO_4^{2-}). We mark this as truly the start of the modern era for ionic liquids. Two years later, Fuller et al. [10] extended this approach to the synthesis of water-insoluble, $[PF_6]^-$ containing ionic liquids as well. Although subsequent authors have suggested numerous refinements on these methods, these basic procedures are still followed today.

Facilitated by these new synthetic tools, the current resurgence of interest in ionic liquids is owed to the realization that, as solvent systems, ionic liquids possess a number of attractive properties. For example, while ionic liquids appear to rival VOCs in the number and types of organic reactions that can be pursued in them, the ionic liquids we discuss in this review have no measurable vapor pressures, obviating evaporative losses to the environment, a fact which offers significant safety, ecological, and economic benefits. Further to this, their vanishingly small vapor pressures make them ideal green engineering solvents allowing for direct distillation of solutes and simple solvent recycle

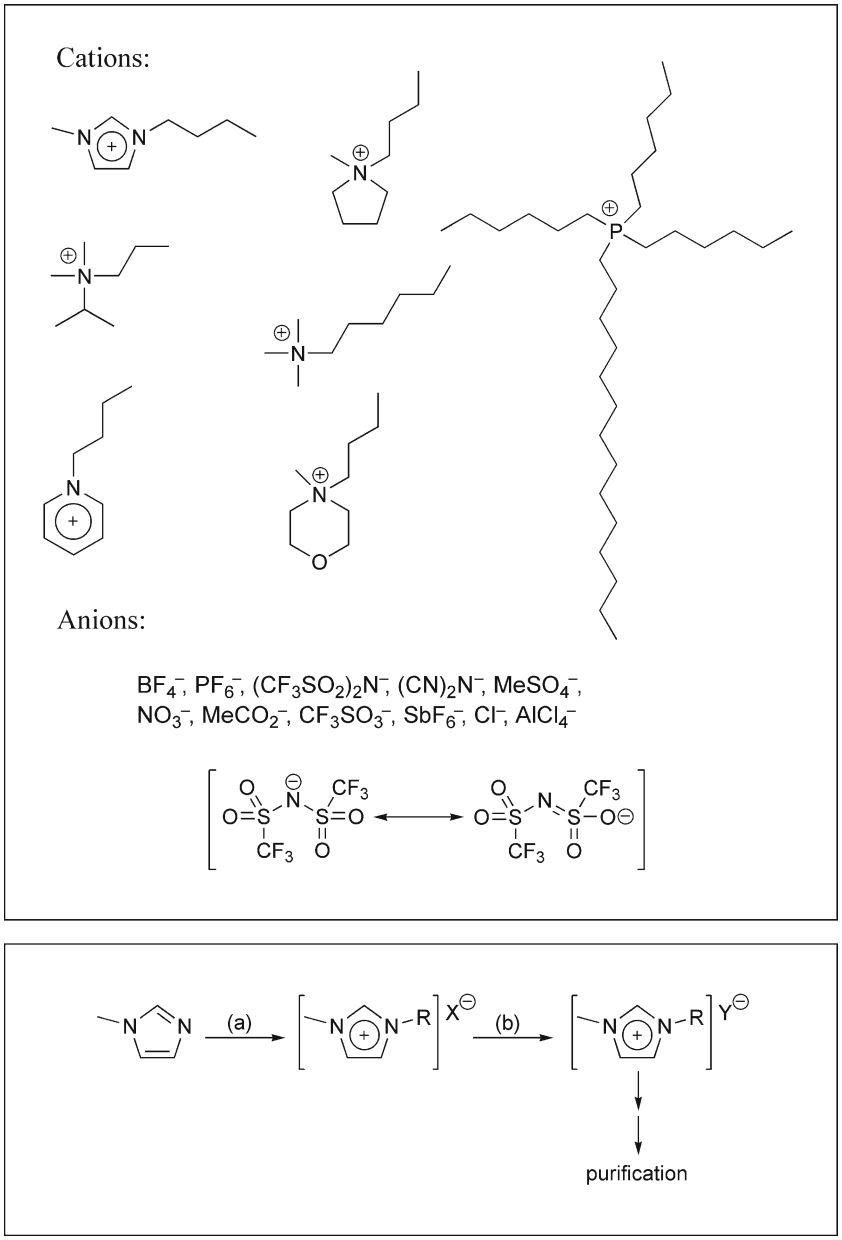

Fig. 1 Examples of cations and anions commonly paired in ionic liquid formulation. Weakly coordinating anions delocalize the negative charge through induction to highly electronegative atoms or by resonance as shown explicitly for the $[Tf_2N]^-$ anion (*upper*). General synthetic strategy for the preparation of ionic liquids using a 1-alkyl-3-methylimidazolium ionic liquid for illustration: (**a**) RX, (**b**) MY (aq.), M=H, Na, NH_4 (*lower*). This basic approach is generally applicable to other classes of cation as well

without VOC production. Indeed, their nonvolatility alone has been a significant factor in the "greening" of ionic liquids. Other essential features common to ionic liquids include a wide electrochemical window (typically, 4–6 V), high conductivity/ionic mobility, broad liquidus range, chemical and thermal stability, and the ability to dissolve a diversity of solute types.

It is also abundantly clear that ionic liquids not only provide a unique solvent in which to carry out chemical transformations but, by systematic alteration in the parent ions, one can tune a number of their solvent properties including viscosity, melting point, density, conductivity, refractive index, polarity, phase equilibria, and water miscibility. Thus, the term "designer solvent", a now-popular honorific coined by Kenneth Seddon, was born. In many respects, however, the design rules and precisely what features are subject to design still need to be fleshed out in much greater detail. Still, ionic liquids *are* "modular" in that for any given parent structure one can, in principle, generate a vast array of possibilities simply by iterative variation in the cation system, its substitution pattern and/or the choice of anion. Indeed, Seddon has remarked that at least a million binary and over 10^{18} ternary salts that qualify as ionic liquids might be possible [11]. While estimates regarding the number of possible ionic liquid systems abound, such estimates are entirely speculative. Regardless, in a practical sense, the variety can truly be considered boundless. Within the last decade, the portfolio of known ionic liquids has greatly expanded from a few dozen to several hundred. Still, the majority of these were reported with little detail beyond

their preparation and with data on their physical properties incomplete or completely lacking. By comparison, about 600 molecular organic solvents find use today with a few dozen, most of these VOCs, comprising the bulk of industrial usage. So, despite this apparent flexibility, at this time the number and variety of well characterized and/or commercial ionic liquids is still very limited compared with molecular organic solvents available to the chemist. This is, of course, a situation that only continued effort will reverse. Even so, given the myriad possibilities for binary combinations alone, clearly a guided search is to be preferred over an Edisonian one.

That the solvent properties of ionic liquids can be changed by modification in the cation and/or anion component is beyond contention, however, at this stage in the game a comprehensive blueprint on how this can be done still does not exist. Moreover, despite the boundless variety possible, in practice, considerations such as cost, toxicity, melting point, viscosity, hydrolytic stability, and purity will limit the choice of useful ionic liquids. Clearly, in aid of this, more data are needed in order to discern precisely what the design rules are for these designer solvents.

Over the last decade or so, the broad research area encompassing ionic liquids has witnessed nearly exponential growth in the number of published papers. What accounts for this unstinting, and indeed growing, popularity? Clearly, the ionic liquid is no longer simply an academic curiosity although it should certainly remain that as well. The recent interest is due to the expectation that ionic liquids, formerly used in specialized electrochemical applications, will find even greater utility as reaction solvents. A grander hope is that ionic liquids will make a significant, lasting and viable contribution to *innovative*, *efficient* and *clean* chemistry, the chemical industry's "Triple Crown".

At this point, a word about ionic liquid nomenclature is helpful. Throughout this review, we will follow the popular bracketed shorthand of the form $[C^+][A^-]$ where C^+ and A^- denote the constituent cation and anion, respectively. Since we will deal exclusively with univalent binary ionic liquids, there is no need to show the charges explicitly. Some cations discussed herein include 1-ethyl-3-methylimidazolium, $[emim]^+$; 1-butyl-3-methylimidazolium, $[bmim]^+$; 1-hexyl-3-methylimidazolium, $[hmim]^+$; 1-octyl-3-methylimidazolium, $[omim]^+$; 1-decyl-3-methylimidazolium, $[dmim]^+$; 1-butyl-1-methylpyrrolidium, $[bmpy]^+$; *N*-butylpyridinium, $[bpyr]^+$; tetradecyltrihexylphosphonium, $[P_{14,666}]^+$. Anions include nitrate, $[NO_3]^-$; hexafluorophosphate, $[PF_6]^-$; tetrafluoroborate, $[BF_4]^-$; bis(trifluoromethane sulfonyl)imide, $[Tf_2N]^-$; acetate, $[Ac]^-$; dicyanamide, $[dca]^-$.

Solvatochromic Probe Studies

Although the opportunity for improving industrial processes is a major driver for basic ionic liquid research, limitations in the detailed physicochemical characterization of these highly promising materials continue to hamper their most efficient utilization. Ironically, it is the boundless experimental space represented by the vast number of potential ionic liquids that actually presents the biggest hurdle in that, as a research community, we can only synthesize and study the properties of a nominal fraction of what is ultimately possible. It is, therefore, important to establish links between features subject to design and more fundamental properties that can be predicted and measured. Properties pursuant to its efficient utilization as a solvent are those that determine how it interacts with a solute of interest. It is also important that realistic comparisons be made between ionic liquids and the molecular solvents they may one day replace. Our ability to predict an ionic liquid composition with a desired set of properties, however, awaits a more fundamental understanding of structure-property relationships. In this respect, fluorescent solutes can serve as very informative probes [12–14] for gaining information about the nature and dynamics of ionic liquids as solvents and for understanding the influence of the completely ionic environment on excited-state species.

Although as chemists we often speak of "solvent polarity" as if it were a single, well-defined quantity, in reality no simple combination of solvent properties can gauge the complex interactions responsible for solvation. In fact, no rigorous theoretical definition for polarity even exists. While early discussions of polarity naively restricted the term to nonspecific electrostatic interactions between solute and solvent, we now appreciate the important, and sometimes dominant, specific interactions that may be present. We will have more to say on this topic later.

Solvatochromic scales of solvent polarity are well-known in organic chemistry for their ability to correlate apparent solvent "polarities" with reaction equilibria and kinetics [1, 2, 15]. Such scales rely on solvent-induced spectral changes to establish the relative strengths of solute–solvent interactions, an approach that has been widely used to address a multitude of research questions in biology, chemistry, materials science, medicine, and physics [1, 13, 14]. Polarities measured in this way are generally more useful than dielectric estimates in that they are sensitive to short-range phenomena not captured in dielectric measurements [16]. There are scores of solvatochromic probes in use today with different empirical scales often ranking solvents somewhat differently. Such disparity is neither surprising nor need it be unduly problematic. Like an investigative reporter in the field, the information "broadcast" by a solvatochromic probe will reflect its own particular sensitivity ("political views") to different solvent attributes such as electronic polarizability, dipole density, and/or hydrogen bonding. This sensitivity is clearly influenced by the molecular structure of the probe as this in turn determines its pK_a, dipole

moment, average site of solubilization, and so forth. In this way, significant effort has been expended toward the design and development of molecular probes selective toward particular solvent properties [14]. Overall, one must understand what interactions are reflected by a given solvent polarity scale and exercise caution when making direct comparisons between scales. Despite this caveat, solvatochromic probe studies of polarity within ionic liquids started to become increasingly popular even during the early stages of ionic liquid research [17, 18]. And while an empirical polarity scale can be a dangerous oversimplification, it can also offer genuinely useful insight into the design of ionic liquid systems. A key example is the work of Dzyuba and Bartsch where a clear correlation was established between $E_T(30)$ and the *endo*/*exo* ratio for Diels–Alder reaction between cyclopentadiene and methyl acrylate in a series of [X-mim][Tf_2N] ionic liquids in which X is a functional group-containing substituent [17].

The emerging potential of computational methods toward studies of solvatochromism in ionic liquids is made apparent by two reports. In the first, Monte Carlo simulations of the pyridinium *N*-phenolate betaine-30 solvatochromic dye in a dozen conventional organic solvents were used to explore the molecular basis for the ever-popular $E_T(30)$ solvent scale [19]. Later, Znamenskiy and Kobrak extended this approach to molecular dynamics simulations of solute–solvent interactions for this same probe in the ionic liquid [bmim][PF_6] [20]. Gas chromatographic and liquid-liquid extraction methods are also widely used to study the thermodynamic properties of pure solvents and solvent mixtures. Although we will not consider such here, progress to date using both chromatographic and spectroscopic approaches toward the study of ionic liquid polarity has been chronicled in a comprehensive review by Poole [21].

Although absorbance-based polarity scales, particularly the $E_T(30)$, find increasing use, in this review we focus primarily on the application of fluorescent probes for such measurements. Not only is fluorescence spectroscopy inherently multidimensional [12] allowing access to nanosecond and faster dynamical information, but its low limits of detection make working at probe concentrations of 10^{-6} M and below trivial. This allows experiments to be conducted under conditions approximating *infinite dilution* where solute–solute interactions can generally be ignored.

Scope of This Review

The goal of this review is to present some concepts of modern molecular fluorescence spectroscopy as they relate to extricating key pieces of information regarding solute–solvent behavior and solute–solvent interaction within ionic liquid systems. Selected examples from the literature are mentioned briefly within each subsection; however, the discussion is not necessarily exhaustive. As carefully as possible, we will summarize the rather limited data that have been published to date in this area and conclude with a very brief discussion of solvent relaxation measurements that have been carried out in a number of laboratories.

It is in no way the purpose of this review to repeat material adequately surveyed elsewhere. For more general information on the field including historical context, synthesis and purification, physical and chemical properties, and applications, the interested reader is directed to conference proceedings and books on the topic published within the last few years [3, 22–32]. As a jump point for browsing the already substantial primary ionic liquid literature out there, we point to the authors of these books, along with many more, as the key contributors to the field at the moment. The field continues to attract talented newcomers, including well-established scientists, from far-ranging disciplines the world over and at such a rate as to make a comprehensive "who's who" list cumbersome and dated, particularly as ionic liquids become even more mainstream.

"Spec-Grade" Ionic Liquids

We stated above that ionic liquids have virtually no vapor pressure, allowing for the direct distillation and even sublimation of products from them. The counterpoint to this is that ionic liquids themselves cannot be purified via simple distillation. While halide-free ionic liquids can be prepared by direct alkylation of a phosphine, amine, pyridine, or azole using dialkyl sulfate or alkyl triflate, for example, the range of ionic liquids accessible by this approach is quite limited. More commonly, ionic liquids are formed using a two-step route involving sequential alkylation and metathesis. This procedure is shown schematically in the lower panel of Figure 1 using the formation of a 1-alkyl-3-methylimidazolium ionic liquid as an example. For complete details on their preparation, readers should consult several excellent volumes on the topic [3, 23, 25–32].

While the chemistry involved is very simple, the early days of ionic liquid preparation began as something of a cottage industry. The tricks of the trade, particularly with regards to producing colorless ionic liquids, have been somewhat guarded. Even established researchers in the field sometimes produce highly colored ionic liquids, however, in our experience, and in accord with the observation of others [33, 34], ionic liquids intended for use in photochemical or spectroscopic studies generally require more careful preparation and purification (i.e., "spec-grade" ionic liquids). Indeed, ionic liquids prepared following highly cited literature procedures often result in deeply colored materials. Although the origins and exact chemical nature of these

colored impurities have yet to be determined, they likely involve oligoamine species and/or thermal or oxidation products thereof. In the course of our initial work in this area, we found that the blank contribution from the ionic liquid solvent itself could be so significant as to make the collection of meaningful spectroscopic data impossible in some cases. Toward this, some basic precautions in the preparation of reliable, spec-grade ionic liquids follow. These methods can be used to prepare spec-grade ionic liquids with minimal interference from absorption above ca. 275 nm. Our motivation is to produce "spectroscopically silent" ionic liquids, however, there is no reason to suspect that ionic liquids applied to catalytic and mechanistic studies do not warrant similarly purified materials under special circumstances. Of course, in particular cases, for example when an anion such as nitrate has substantial intrinsic absorbance in the UV, this will *not* be possible.

(i) Organic starting materials should be purified following established literature procedures [35] although we have generally found it unnecessary to purify lithium salts prior to anion exchange reactions. We further suggest that alkyl bromides be *doubly* distilled prior to use.

(ii) The alkylation step should be carried out in an inert atmosphere using standard Schlenk line techniques or freeze-pump-thaw degassing. It is important to keep the temperature as low as possible. After combining the reagents neat under stirring with the reaction vessel immersed in an ice bath, all associated glassware should be carefully wrapped with aluminum foil to retard any photolytic or photo-oligomerization processes. After several hours, the reaction is warmed to room temperature after which the reaction continues for a full week. In order to achieve good conversion yields, an alkyl bromide added in excess should be used as the alkylation agent. The washed and filtered halide salt is recrystallized from acetonitrile or acetone to yield a white crystalline powder upon overnight drying in a vacuum oven at 40 °C. This step may be repeated as necessary. If there is *any* tinge, the halide salt is immediately dissolved in water and stirred with decolorizing carbon for several days. The aqueous solution is then centrifuged (15 min, 5000×*g*) followed by filtration using a 0.45 μm nylon syringe filter. This step is repeated several times. *It is essential that the least tint of color be removed at this step as such becomes virtually indelible following metathesis*. We avoid the use Celite® as this was found to reintroduce impurities that absorb and/or fluoresce.

(iii) If available, we recommend lithium salts over their ammonium analogs as the anion source and discourage the use of free acid for anion metathesis. Metathetic by-product salts such as lithium bromide can be efficiently removed from water-immiscible ionic liquids by iterative liquid-liquid extraction with water. In practice, this should be done until the extractant tests negative for bromide with silver nitrate followed by at least five additional washes. The final halide content should be quantified using an ion-selective electrode, ion chromatography, electrochemistry, argentometric titrations (Volhard or Fajans methods), or additional spectrophotometric or fluorimetric techniques.

(iv) Following halide removal, if the as-prepared ionic liquid exhibits very slight coloration it can sometimes be removed by elution on a short column of preequilibrated activated carbon terminated with neutral activated alumina (150 mesh, 58 Å). Be warned, while this step can lower the water content of the ionic liquid, significant amounts of material are irretrievably retained on the column *and* this step cannot always salvage a hued ionic liquid in the first place.

At this point, the ionic liquid should be relatively pure and color-free, however, a "water-immiscible" ionic liquid will still contain as much as 1–3 wt % water. We recommend preliminary drying on a vacuum line for several days without heating. Smaller volumes of ionic liquid should then be individually dried by heating at 60–70 °C under high vacuum (<0.1 mbar) for at least 48 h followed by storage in vacuum-sealed vials, a desiccator, or a dry-box. We have found this to be an effective way to ensure efficient water removal with residual levels of ca. 5×10^{-3} M, a level which may be considered scrupulously dry [36]. We will discuss some of the implications of ionic liquid water content in what follows.

UV–vis spectra for [bmim][BF_4] prepared following these methods versus two different lots of a commercial grade of [bmim][BF_4] from a single vendor are displayed in Figure 2. We note that, visually, sample A (spec-grade or grade "A") was completely transparent and indistinguishable from ethanol to the eye, B had a subtle hint of color, and C was distinctly yellow. By following steps (i)–(iv) outlined above, we were able to extend the optical transparency of this ionic liquid down to ca. 240 nm allowing for direct excitation of UV excitable probes dissolved in the ionic liquid; the weak band near 244 nm arises from π,π^* absorption from the imidazolium ring itself. This UV cut-off was confirmed by circular dichroism (CD) studies in the near-ultraviolet region as well. In our experience, although these steps are both tedious and time-consuming, this level of purity is absolutely essential for many photophysical studies in the ultraviolet. Specifically, we have found that with conspicuously colored ionic liquids inner filtering/self-absorption is a serious impediment to obtaining correct, useful fluorescence spectra at wavelengths below 350 nm.

While primary inner filtering can sometimes be ignored at a constant excitation wavelength [37], significant re-absorption of emitted fluorescence (secondary inner filter effects) invariably leads to wavelength-dependent artifacts in the ultraviolet region. Secondary inner filter correction factors, f_{sec}, calculated for the three grades of [bmim][BF_4] are provided in the lower panel of Figure 2 (note that f_{sec} equals unity at A=0). As illustration of the effects of such inner filtering, the thusly corrected and normalized emission spectra generated by applying these secondary absorption correction profiles to a simulated parent spectrum for a prototypical single tryptophan protein are inset in the lower panel. While the spectrum calculated using correction profile "A" perfectly overlays that of the original spectrum, use of correction profile "C" manifests in artificial spectral narrowing (FWHM decreases from 58 to 47 nm), a change in peak shape/symmetry, and an overall blue shift (centers-of-gravity (COG) / nm: A=340.6; C=336.4). While this may appear to be a trivial effect to the uninitiated, one must bear in mind three things. Firstly, changes in the tryptophan

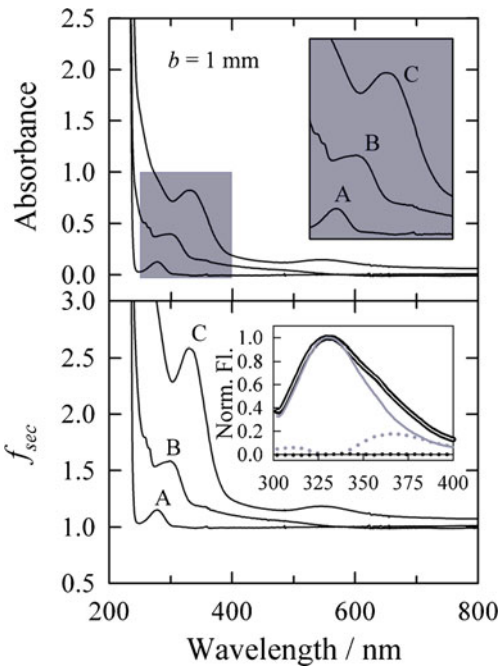

Fig. 2 UV–vis absorption spectra for [bmim][BF_4] using ionic liquid prepared using methods refined in our laboratory (**a**) or material obtained from two different lots from a single commercial vendor (**b** and **c**) for a 1-mm pathlength. The inset shows an expanded view of the shaded 250 to 400 nm region (*upper*). The corresponding secondary inner filter correction curves (*lower*). In the inset is shown a hypothetical single-Trp protein emission spectrum (*black curve*) and normalized emission profiles based on applying inner filter correction curves A and C to this spectrum (white and gray profiles, respectively). The black and gray dotted curves in the inset are the difference spectra between the parent spectrum and the corrected spectra based on f_{sec} profiles A and C, respectively. These results illustrate the kind of self-absorption bias that may easily arise from typical absorption values for ionic liquids prepared using conventional means. See text for additional details

residue emission maxima or COG of only a handful of nanometers can be telling in studies of protein conformation and unfolding [38, 39]. Second, these correction factors were estimated for a square cell with a pathlength of only 1 mm. A typical 1-cm^2 cell will result in considerably more bias as will the use of more absorbing ionic liquid samples. Finally, ionic liquids with even higher correction factors are not uncommon. Despite careful attempts at correcting such spectra, in some instances we point out that significant luminescent backgrounds from more problematic ionic liquids may preclude spectroscopic studies altogether.

The wide scatter in some physical properties (e.g., density, conductivity, viscosity) reported for ionic liquids can be largely attributed to the effects of impurities, particularly water [36]. Although water miscibility is dictated largely by anion choice, virtually all known ionic liquids are hygroscopic and for this reason all ionic liquids can be said to contain some greater or lesser amount of water. Although dialkylimidazolium ionic liquids paired with halide, ethanoate, nitrate, dicyanamide, or trifluoroacetate are frequently water miscible, those containing either hexafluorophosphate or bis(trifluoromethane sulfonyl)imide generally form a biphase with water. Even these latter "hydrophobic" ionic liquids will contain a few wt % water upon prolonged exposure to moist laboratory air; for example, [bmim][Tf_2N] saturates at about 1.4 wt % water [3]. On a molar basis, this is a substantial amount of water, in some cases more than 1.0 M. The presence of water influences the physical properties of the ionic liquid and may also affect reaction rates by occupying catalytic coordination sites or by modulating the bulk viscosity. One must also be alert to the possible impact of trace amounts of water on hydrolysis rates, reactant and product solubility, decomposition pathways, product distributions and by-products. When it is important to precisely know the water content within an ionic liquid, this should be determined using Karl Fischer coulometry. In any case, the approximate level of water should be determined for which infrared or near-infrared (NIR) absorption, as well as cyclic voltammetry and ^{1}H NMR, will suffice.

Many of the effects induced by water may also be directly or indirectly reflected by changes in the microenvironment surrounding a fluorescent solute dissolved within an ionic liquid. For example, we have reported a fluorimetric method to estimate the water content of several 1-alkyl-3-methylimidazolium ionic liquids in the 0 to 25 mol % water regime (Figure 3) [40]. Controlled addition of water to ionic liquids acts to lower the bulk viscosity of the solvent proper [36]. We have found that this effect is also mirrored microscopically in that higher water contents result in apparent increases in the rate of intramolecular cyclization for excimer-forming 1,*m*-bis(1-pyrenyl)alkanes (m=3, 10) dissolved in the ionic liquid. Moreover, surprisingly good linear correlations were observed between the excimer-to-

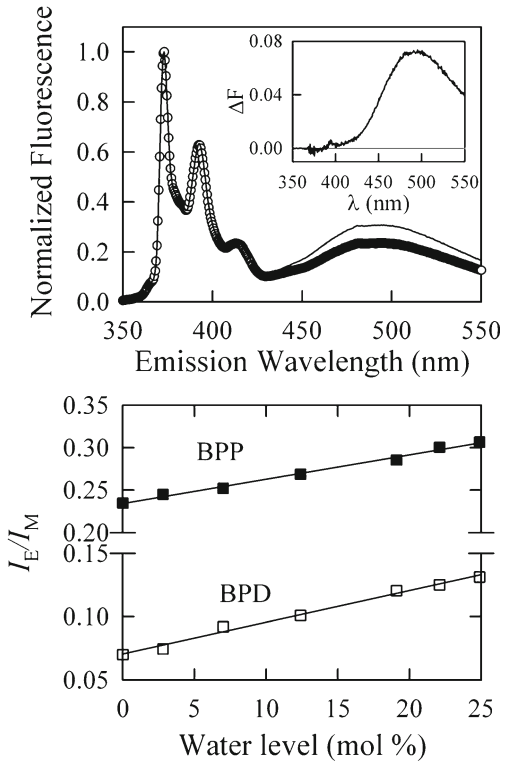

Fig. 3 Steady-state emission spectra for 1,3-*bis*(1-pyrenyl)propane in [emim][Tf_2N] at water contents of "0" (○) and 25 mol % (——) normalized to the highest energy emission peak. In the inset is shown the difference spectrum, consistent with dynamically formed excimer (*upper*). The linear relationship between excimer-to-monomer intensity ratio and mol % water for 1,3-*bis*(1-pyrenyl)propane (BPP, m=3) and 1,10-*bis*(1-pyrenyl)decane (BPD, m=10) in the same ionic liquid (*lower*)

monomer intensity ratio (I_E/I_M, a reflection of the local *microfluidity*) and the mole fraction of water present in the ionic liquid, i.e., the coefficient of determination, R^2, lies between 0.988 and 0.997 [40].

Polarity Determinations within Ionic Liquids

The IUPAC recommendation is that solvent polarity must include the *sum of all possible, non-specific and specific, intermolecular interactions between the solute ions or molecules and solvent molecules, excluding such interactions leading to definite chemical alterations of the ions or molecules of the solute* [41]. The complex interplay of forces including Coulombic interactions, directional interactions between dipoles, quadrupoles or multipoles, inductive, dispersive, hydrogen-bonding, ionic/charge transfer and hydrophobic interactions, conspire to determine a solvent's effective polarity and ultimately its potential toward a target application. Because of the complex nature of these interactions, single macroscopic physical parameters like static dielectric constants, dipole moments, and refractive indices cannot sufficiently describe solvent polarity or solvent strength. This limitation coupled with the lack of adequate theory has led to the introduction of a host of empirical solvent polarity scales based on solvent interactions with model solvatochromic probes [1, 42–46]. In 1958, Kosower was the first to construct an empirical polarity scale, the *Z*-scale, based on the ground-state charge transfer absorption band of 4-methoxycarbonyl-1-ethylpyridinium iodide. Among the more popular empirical polarity scales used over the years to characterize solvent polarity are the *Y*-scale introduced by Winstein, the Grunwald parameter [(ε–1)/(2ε+1)], the *Py*-scale devised by Dong and Winnik, Reichardt's $E_T(30)$ scale, Gutmann's donor and acceptor numbers (DN/AN), and the linear solvation energy relationship (LSER) developed by Kamlet and Taft.

While common molecular organic solvents are generally more limited in the scope of interactions possible with a dissolved solute, ionic liquids are capable of a far wider range of interactions. It is also important to bear in mind that even a "pure" anhydrous ionic liquid (if such exists) is still a binary solvent mixture of sorts. That is, on a microscopic level, within a neat ionic liquid both the cation and the anion may have their own distinct and specific interactions with a given solute. The interaction between the cationic and anionic components of the ionic liquid may also be the genesis of a third unique "environment". Further complexity is suggested by mounting evidence that such cation–anion interaction actually *moderates* their individual interactions with a solute under study. Clearly, addition of a co-solvent modifier or a second ionic liquid phase will result in a dizzying number of convoluted interactions and possible environs among which a solute may partition.

In the five sub-sections that follow, we will survey recent solvatochromic studies of solvent polarity in ionic liquid systems of increasing complexity. We will begin with "neat" ionic liquid systems and proceed to simple co-solvent modified ionic liquids, binary ionic liquid mixtures and conclude with CO_2 modified ionic liquids followed by surfactant modified ionic liquids.

Neat Ionic Liquids

Nearly two decades ago, Huppert and coworkers initiated studies aimed at understanding solvation processes within molten tetra-*n*-alkylammonium salts of the form [R_4N][X], for R=propyl, butyl, hexyl, octyl, decyl, and dodecyl and X=hydrogen sulfate or perchlorate. In one such study, these authors investigated the effects of cation size (values for effective radii ranged from 4.4 to 7.0 Å) on the static emission spectrum of the popular positive solvatochromic probe coumarin 153 (C153) dissolved in molten salts held a

few degrees above their melting points (105–170 °C) [47]. A hypsochromic (blue) shift in probe emission was observed with an increase in the alkyl chain length, consistent with the greater hydrophobic character of the melt as a result of chain elongation. Correlating the relative position of the fluorescence band maxima for C153 to the normalized $E_T(30)$ scale, E_T^N (this scale ranges from $E_T^N=0.00$ for nonpolar tetramethylsilane to $E_T^N=1.00$ for water) suggests a monotonic decrease in polarity from a value similar to water ($E_T^N=0.93$) for tetrapropylammonium hydrogen sulfate to a low polarity akin to tetrahydrofuran ($E_T^N=0.22$) for the tetradecylammonium perchlorate.

Bonhôte et al. were the first to report on solvatochromic studies of polarity within an ambient temperature ionic liquid [48]. Specifically, they used pyrene-1-carboxaldehyde (PyCHO) and pyrene in order to compare the solvent properties of [emim][Tf_2N] with common organic solvents [48]. PyCHO belongs to a class of neutral probe molecules whose emission properties change due to a shift in the nature of the emitting state upon increasing solvent polarity. Kalyanasundaram and Thomas found that, barring a few exceptions, the fluorescence maximum of PyCHO varies linearly with the static dielectric constant, ε, over a broad range spanning all protic solvents (ε = 10–80) [49]. The mechanism of this photophysical response can be simply understood. Briefly, PyCHO has two types of low-lying excited singlet states (n,π* and π,π*), both of which show emission in fluid solution. In nonpolar solvents such as *n*-hexane, the emission from PyCHO is highly structured and weak (quantum yield less than 10^{-3}) arising from the n,π* state. On increasing the polarity of the medium, however, the π,π* state is brought below the n,π* state via solvent relaxation to become the emitting state. This manifests in broad, moderately intense emission (for example, the emission yields for PyCHO in methanol and 1:1 methanol:water are 0.15 and 0.69, respectively) that redshifts with increasing ε. Bonhôte et al [48] found that PyCHO exhibited an emission maximum of 431 nm in [emim][Tf_2N], a value close to that observed in 1-hexanol (440 nm). This, coupled with the well-structured absorption spectrum of PyCHO in [emim][Tf_2N] suggests a solvent environment with ε below 10. This apparently low ε is quite surprising given the fact that the hydrogen atom appended to C(2) of the imidazolium ring is highly polarized and capable of engaging in hydrogen bonds with PyCHO. This apparent inconsistency may be reconciled as follows. If the solvent relaxation kinetics are not prompt relative to the S_1 lifetime, the emitting state will not be fully relaxed and, thereupon, the steady-state emission frequencies *will not* provide a true measure of the equilibrium solvation energetics. It is therefore important that the slow relaxation dynamics within ionic liquids not be overlooked in such studies.

Bonhôte et al. [48] also used pyrene to gauge the polarity within [emim][Tf_2N]. In pyrene, solvent-induced perturbations of the π-electronic orbitals by Herzberg–Teller symmetry distortions influence the B_u^2 and B_u^1 interstate coupling efficiency, resulting in a solvent-dependent I_1/I_3 emission band ratio between the solvent sensitive 0–0 band (band 1, ca. 373 nm) and the solvent independent band 3 near 384 nm [50–54]. For pyrene dissolved in [emim][Tf_2N], Bonhôte et al. determined an I_1/I_3 ratio of about 1.18, a value close to that of ethanol [48]. We will take this opportunity to point out a misconception held by some researchers regarding the use of pyrene I_1/I_3 values. That is, while such values are highly reproducible for a given instrumental configuration, often with an estimated error of 0.5 % or better, there will be significant variability in I_1/I_3 values from different labs depending on the optical set-up used for their measurement.

In another study, Aki et al. estimated the polarity of the ionic liquids [bmim][PF_6], [omim][PF_6], [bmim][NO_3], and [bpyr][BF_4] using the relatively small, neutral fluorescent probes 4-aminophthalimide (4-AP) and 4-(*N*,*N*-dimethylamino)phthalimide (4-DAP) [55]. Expressed in terms of the intramolecular π,π* charge-transfer absorption energy of Reichardt's 2,6-diphenyl-4-(2,4,6-triphenyl-1-pyridinio) phenolate which forms the basis of the $E_T(30)$ scale, the emission maxima of 4-AP and 4-DAP provided general measures of the relative solvent strengths of these four ionic liquids. From these studies, it was found that the equivalent $E_T(30)$ values for the ionic liquids lie in the range spanned by polar protic solvents like short-chain alcohols. Specifically, it was determined that both [bmim][PF_6] and [bmim][NO_3] exhibited a polarity similar to ethanol. Furthermore, the emission maximum of 4-DAP in these ionic liquids was nearly identical, implying that anion exchange from $[PF_6]^-$ to $[NO_3]^-$ has little effect on the micropolarity experienced by this probe. In comparison, the apparent polarity of [omim][PF_6] was intermediate between that of acetonitrile and propan-2-ol while [bpyr][BF_4], the most apolar of these ionic liquids, exhibited a micropolarity close to that of acetonitrile. It was also found that more rigorous drying of [bmim][PF_6] under high vacuum at 75 °C for 24 h significantly changed the equivalent $E_T(30)$ polarity from an environment similar to ethanol to one similar to propan-2-ol.

Expanding on this work, Pandey and coworkers used several fluorescent probes to further explore the micropolarity within the ionic liquid [bmim][PF_6] [56]. In addition to pyrene and PyCHO discussed above, the authors also used the probes dansylamide and Nile Red. A brief word about each of these fluorescent probes is in order. The dansyl (5-dimethylaminonaphthalene-1-sulfonyl) moiety is very solvent sensitive, the Stokes shift ($\bar{\nu}_{abs} - \bar{\nu}_{em}/\mathrm{cm}^{-1}$) and quantum yield being strong functions of the solvent dipolarity [57]. Nile Red is a positive solvatochromic probe whose absorption, excitation, and emission maxima all red shift with increasing solvent polarity [58, 59]. Each of these fluorophores was selected to probe different solvent

properties of the ionic liquid and, as such, the polarity reported by a given spectroscopic probe will vary. That is, certain probe–solvent interactions may be favored, causing various probes to perceive differently the components of a solvent mixture. For this reason, when we state that a given ionic liquid is "like" ethanol, for example, implicit in this claim is that this similarity may reflect highly specific solute–solvent interactions. For example, Taft and Kamlet determined that about two-thirds of the shift in transition energy for the $E_T(30)$ dye could be assigned directly to specific interactions with the phenoxide oxygen atom [45]. It was thus postulated that for protic solvents the $E_T(30)$ scale is largely a measure of hydrogen bond donor strength, the Kamlet-Taft α-value. Fluorescent probes have the further complication that the position of the emission maximum may not reflect a fully relaxed excited state prior to emission, as stated above. The corollary to this, of course, is that probes with radiative rates in the 10^8 s^{-1} regime may be used to follow the evolution of the solvation process (i.e., *solvent relaxation*) within ionic liquids.

Pandey and coworkers reported a Stokes shift of ca. 9900 cm^{-1} for dansylamide in [bmim][PF_6], a value statistically equivalent to the value in acetonitrile and slightly lower than that determined in a number of protic solvents [56]. Of course, solvent relaxation is likely to be slowed somewhat in the ionic liquid. Consequently, 90 wt % glycerol in water—a solvent system that affords a viscosity similar to neat [bmim][PF_6] at 20 °C or roughly 300 cP—was also studied. The Stokes shifts observed for dansylamide in 90 wt % glycerol in water and pure water (11450 and 12700 cm^{-1}, respectively) accord with incomplete solvent relaxation within [bmim][PF_6], suggesting a true dipolarity in the vicinity of the lower alkanols. Results for pyrene are also suggestive of a dipolarity within [bmim][PF_6] similar to acetonitrile but, using this probe, the polarity is ranked significantly higher than methanol, ethylene glycol, or even 90 wt % glycerol in water. Similarly, the excitation and emission maxima for Nile Red dissolved in [bmim][PF_6] were red shifted by about 37 and 26 nm, respectively, relative to the values in methanol. In fact, only aqueous solutions yielded comparable excitation and emission maxima. The emission spectrum of PyCHO dissolved in [bmim][PF_6] was significantly blue shifted relative to spectra measured in any of the polar protic solvents studied, ranging from a 21 nm (vs. ethanol) to a 47 nm blue-shift (vs. water). On the other hand, the PyCHO emission maxima in acetonitrile and DMSO were blue shifted approximately 10 nm from the observed maximum in [bmim][PF_6]. From this, one may infer a static dielectric constant below 10 for [bmim][PF_6]. However, in this interpretation, the effects of solvation kinetics on the observed emission profile are not accounted for. Indeed, considering the high viscosity of a typical ionic liquid coupled with the short PyCHO singlet excited-state lifetime (1.95 and 1.90 ns in methanol and 1-propanol, respectively) [49], such effects may result in significant underestimation of ε. In fact, incomplete solvent relaxation will almost certainly be the rule rather than the exception for fluorescent species with lifetimes less than about 10 ns. Taken together, these results suggest a range of apparent polarities inferred from different probes and suggest the utmost caution be used in drawing conclusions based on steady-state results, especially when employing short-lived probes. This apparent incongruity is, in fact, completely understandable by considering the effects of the temporal evolution of the emission spectrum for such probes. In this way, excited-state intensity decays are useful not only for correcting such sources of bias in "polarity" assignments but also for elucidating the kinetics of solvation for a dipolar fluorophore dissolved within an ionic liquid. This topic will be addressed in some detail in the forthcoming section Transient Solvation in Ionic Liquids.

The polarity of another class of ionic liquids, the saturated quaternary phosphonium ionic liquids, was evaluated by Weiss and coworkers [60]. In this work, the relative polarities of five methyl-tri-*n*-decylphosphoniums coupled with bromide and chloride (anhydrous and monohydrate) as well as nitrate, were determined using the probes Nile Red and 1,1-dicyano-2-[6-(dimethylamino)naphthylen-2-yl]propene (DDNP). The monohydrates were found to form smectic A_2 phases persisting below room temperature while the nitrate salt became liquid crystalline only above room temperature. In contrast, the anhydrous salts remain soft solids up to their isotropization temperatures. At this point, one should note that the ordering of these ionic liquid crystals is a significant departure from the "isotropic" ionic liquids discussed thus far. These researchers proposed a partially interdigitated ionic liquid-crystalline packing arrangement consisting of lipidic layers formed from *n*-decyl chains separated by ionic planes composed of phosphonium headgroups and associated anions. Results based on the absorption of Nile Red, expressed in molar transition energies, E_{NR}, reveal that methyl-tri-*n*-decylphosphonium ionic liquids (E_{NR}/kJ mol^{-1}=220.9–228) [60] are less polar than their 1-alkyl-3-methylimidazolium counterparts (E_{NR}/kJ mol^{-1}=215.1–219.2) [59] with the anhydrous bromide salt exhibiting the lowest polarity. Based on these results and lamellar spacings calculated from low-angle X-ray diffraction patterns, it was concluded that Nile Red does not reside within the ionic planes of the liquid-crystalline or layered solid phases. The authors infer, based on emission maxima, that DDNP was similarly incorporated within the phosphonium solid and liquid-crystalline phases, reporting an average polarity somewhat lower than acetonitrile. They also noted a substantial shift in DDNP emission spectra (9–12 nm) to longer wavelengths as the excitation wavelength was increased. This feature was ascribed to site heterogeneity, however, a

more likely explanation is a simple *red-edge excitation shift* resulting from selective excitation of fluorophores with a relaxed solvent configuration within the solid and liquid-crystalline phases. This proposal is consistent with the increase in emission wavelength as the temperature is raised. The origins of such behavior form part of the subject of the final segment of this Review.

In a later investigation, Samanta group studied the behavior of the fluorescence microviscosity probe 9-(dicyanovinyl) julolidine (DCVJ) in seven imidazolium ionic liquids at 10–60 °C [61]. The microviscosities estimated from the linear dependence of the logarithm of fluorescence quantum yield on the logarithm of the bulk viscosity in various conventional solvents turned out to be significantly different from the directly measured bulk viscosities of the ionic liquids studied. These results pin-pointed at the important role of free volume around the probe in dictating the non-radiative deactivation rate or the fluorescence efficiency of DCVJ dissolved in ionic liquids. Nagasawa et al. investigated the temperature dependence of the fluorescence behavior of 9,9'-bianthryl (BA) in imidazolium ionic liquids [62]. As is common in normal polar solvents, they observed that the emission peak of BA in ionic liquids shifted to longer wavelengths with decreasing temperature in the regime of ambient and higher temperatures. On the contrary, at temperatures below 290 K, the emission peak shifted to shorter wavelengths with decreasing temperature. The authors concluded that the origin of the blue-shifted emission at lower temperatures was due to fluorescence from the un-relaxed charge-transfer state. The time-resolved fluorescence results confirmed that the charge separation process of BA in ionic liquids occurred prior to the nanosecond fluorescence red-shift due to the slow solvation process in the charge transfer state. The fluorescence behavior of another probe, 4-(*N*,*N*′-dimethylamino)benzonitrile, was also studied in ionic liquids as a function of temperature and excitation wavelength [63]. The nature of the locally excited (LE) and the intramolecular charge transfer (ICT) states of the probe (relative intensities of the two emission bands and the peak position of the ICT emission) was found to be consistent with the viscosity and polarity of the ionic liquids. Temperature dependent studies showed a blue shift of the ICT emission peak with lowering of temperature, indicating that the emission occurs from an incompletely solvated state of the probe. Excitation wavelength dependence of the emission behavior was observed and was attributed to the microheterogeneity of the ionic liquid media. Wu et al. synthesized three perylene tetracarboxylic diimide (PDI) fluorescence probes, *N*,*N*′-di(2-*N*″,*N*″-dimethylamino)ethylperylene-3,4:9,10-tetracarboxylic diimide (1), *N*,*N*′-di(2-*N*″,*N*″-dimethylamino)propylperylene-3,4:9,10-tetracarboxylic diimide (2), and *N*,*N*′-dicyclohexyl-1,7-pyrrolidinylperylene-3,4:9,10-tetracarboxylic diimide (3) and studied their fluorescence behavior in ionic liquids [64]. The intramolecular photoinduced electron transfer from dimethylamine to PDI in 1 and 2 was found to be efficiently hindered because of the solvation of ionic liquids. A two-conformation mechanism for the PET in 1 and 2 was proposed by the authors to explain the results of the fluorescence lifetime measurements. Interestingly, the solvating power of ionic liquids to 3 was found toward be similar to that of a normal polar organic solvent with polarity greater than that of DMF. The fluorescence behavior of crystal violet lactone (CVL), a probe that exhibits dual fluorescence from two different electronic states, was studied in six different ionic liquids by the Samanta group [65]. It was demonstrated that the dual fluorescence of CVL could be controlled by appropriate choice of the ionic liquid. Specifically, the dual fluorescence of CVL was observed in pyrrolidinium ionic liquid, whereas the probe was found to exhibit a single fluorescence band in an ammonium ionic liquid. Further, the second emission could barely be seen in 1,3-dialkylimidazolium ionic liquids, although dual fluorescence was clearly visible in 1-butyl-2,3-dimethylimidazolium ionic liquid. The authors explained these contrasting results by taking into account the hydrogen bonding interactions of the 1,3-dialkylimidazolium ions (mediated through the C(2)-hydrogen) with CVL and the individual viscosity of the ionic liquids.

In an attempt to estimate and understand the polarity of hydroxyl ionic liquids, a series of ionic liquids based on hydroxyethyl-imidazolium cation with various anions ($[PF_6]^-$, $[Tf_2N]^-$, $[ClO_4]^-$, $[dca]^-$, $[NO_3]^-$, $[Ac]^-$, and Cl^-) and the corresponding non-hydroxyl ionic liquids were investigated by fluorescence probes [66]. Except [emim][Ac], as expected, most of the non-hydroxyl ionic liquids exhibited anion-independent polarity, whereas the polarity of the hydroxyl ionic liquids covered a rather wide range and showed strong anion dependence. These authors have suggested classifying the hydroxyl ionic liquids into three groups, namely, acetate-based hydroxyl ionic liquids, hydroxyl ionic liquids containing anions $[NO_3]^-$, $[dca]^-$, and Cl^-, and hydroxyl ionic liquids containing anions $[PF_6]^-$, $[Tf_2N]^-$, and $[ClO_4]^-$. In an interesting study, fluorescence of fullerene C70 in ionic liquids was investigated by Martins and coworkers [67]. These researchers showed that pristine fullerene C70 could be solubilized in imidazolium, ammonium and phosphonium based ionic liquids having long alkyl chains (C8 or higher). The fluorescence properties of fullerene C70 were found to be similar to those displayed in conventional polar solvents except in ionic liquids containing chloride as the counter ion. Chloride ions completely quenched the fluorescence of fullerene C70. The steady-state fluorescence emission of a model metalloporphyrin, ZnTPP, was also used to investigate properties of ionic liquids [68]. Using a highly purified sample of the common ionic liquid, $[bmim][PF_6]$, it was revealed that S_2-S_0 emission resulting from Soret-band excitation was similar to that

observed in molecular solvents of the same polarizability. The Dyson group utilized an internal fluorescent probe based on anthracene to evaluate the cation–anion interactions in imidazolium salts [69]. For this purpose, a series of fluorescent imidazolium-based salts containing cation $[AnCH_2MeIm]^+$ (An=anthracene and Im=imidazolium) with Cl^-, $[BF_4]^-$, $[PF_6]^-$, $[TfO]^-$, $[dca]^-$, $[Tf_2N]^-$, or $[PhBF_3]^-$ anions were synthesized. Fluorescence emission analysis of these salts dissolved in acetonitrile showed that the fluorescence varied significantly according to the nature of the anion, and correlated to the extent of ion pairing present in the solution.

To explore whether the bimolecular electron transfer reaction rates in ionic liquids are anomalously high as reported earlier, in an important recent publication, the Maroncelli group used steady-state fluorescence along with picosecond time-resolved emission spectroscopy to monitor the bimolecular electron transfer reaction between the electron acceptor 9,10-dicyanoanthracene in its S_1 state and the donor *N*,*N*-dimethylaniline in a variety of ionic liquids and several conventional solvents [70]. These authors studied the fluorescence quenching associated with this system in detail to understand why rates reported for similar diffusion-limited reactions in ionic liquids sometimes appeared much higher than expected. Consistent with previous studies, Stern–Volmer analyses of the steady-state and lifetime data provided effective quenching rate constants that were 10 to 100-fold larger than simple predictions for diffusion-limited rate constants in ionic liquids. However, similar departures also observed in conventional organic solvents having comparably high viscosities indicated that this behavior was not unique to ionic liquids. By using a more complete analysis of the quenching data, the authors were able to reveal the reason behind this observation. The authors have suggested that the high viscosities typical of ionic liquids emphasize the transient component of the diffusion-limited reactions, which rendered the interpretation of rate constants derived from Stern–Volmer analysis ambiguous. It is demonstrated that using a more appropriate description of the quenching process enabled satisfactory fits of data in both ionic liquids and conventional solvents using a single set of physically reasonable electron transfer parameters.

Co-Solvent Modified Ionic Liquids

The desire to expand the utility of ionic liquid systems and to adjust their physicochemical properties has prompted several research initiatives in the area of mixed solvent systems. In particular, recent emphasis has been placed on understanding how the use of miscible co-solvents such as water or ethanol influences the physicochemical properties of the solvent. Such changes offer a degree of control over key solvent parameters leading to possible engineering advantages and/or significant benefits in their use as solvents for extractions, separations, and reactions. From a green perspective, efficient product recovery and reuse without generating secondary waste is also of key importance. In this regard, the efficiency of clean extraction processes including supercritical fluid stripping, distillation, and pervaporation is also likely to be influenced by such changes.

All known classes of ionic liquid exhibit some degree of hygroscopicity and, as such, water may be viewed as the most ubiquitous and influential "impurity" in materials not subjected to exigent drying conditions. Consider, for example, [bmim][PF_6], the most prevalent ionic liquid in the open literature. It is noteworthy that the $[PF_6]^-$ anion is a poor hydrogen-bond acceptor and, consequently, water should not partition into this ionic liquid. And yet, the water content of this "hydrophobic" ionic liquid has been reported to be 1.2–2.3 wt % at saturation, a significant amount on a molar basis (16–27 mol %). This residual water may occupy catalytic coordination sites and can otherwise affect hydrolysis rates, reactant and product solubility, decomposition pathways, and product and byproduct distributions. Conversely, a certain water activity is thought to be required for maintenance of enzyme activity within ionic liquids. Furthermore, the considerable scatter in the physical data for ionic liquids found in the literature (absolute viscosity, for example) has often been attributed to disparity in the water content which frequently goes unreported. Friend or foe, the presence of even small amounts of water in an ionic liquid clearly influences its physical properties including viscosity, conductivity, and density. For these reasons, it is critical that the water content of an ionic liquid be accurately known and that the impact of water content on the resulting solvent capacity be properly understood. Spectroscopic evidence gained from select solvatochromic species solubilized within an ionic liquid can reveal key information about the immediate surroundings such as perturbations in the local dipolarity, hydrogen bonding, or microviscosity. This zone of interrogation around a solute molecule, the *cybotactic region*, includes both the first solvation shell and the transition region and will be strongly influence by the presence of water. These data are useful not only for quantifying the water content of an ionic liquid but also for establishing a rubric for tailoring an ionic liquid to fit an intended application.

As we stressed earlier, the solvent sensitivity and the nature of the specific interactions with the ionic liquid can vary significantly depending on the experimental probe used. In particular, volume and hydrogen-bond acceptor terms appear to be the most important predictors of the overall solvating environment. Whatever the probe, an interesting possibility in any solvent mixture is the observation of *preferential solvation*. For example, there may exist in a binary solvent system a selective enrichment of one of the two solvent components surrounding a probe solute relative to

the bulk composition. Such local mole fraction excursions reflect specific interactions between the probe and individual components within a mixture and are of both pure and applied interest. For, example, knowledge of these interactions can be used advantageously to facilitate differential separations or in azeotrope-breaking for extractive distillation. One should also be mindful of the fact that solvent molecules within the cybotactic zone are acted upon by the field of the solute itself. For instance, "dielectric enrichment" is common in the neighborhood of a dipolar solute.

By definition, preferential solvation exists whenever the local solvent composition deviates from the bulk composition. Assuming that solvent–solvent association may be neglected, the idealized spectral response, R, in a binary solution (A+B) is simply a mole fraction weighted sum (volume fraction is sometimes used instead) of the spectral responses in the pure solvents [71–74].

$$R = X_A R_A + (1 - X_A) R_B \tag{1}$$

In Eq. (1), X_i is a mole fraction of the i^{th} solvent in the bulk and R_i is the spectral response of the probe in that pure solvent. In this way, deviations between the measured response, R_{obs}, and the response assuming ideal mixing, expressed as an excess function (R_{obs}–R), can often reveal a local enrichment of one component or changes in solvent–solvent interaction. Importantly, because preferential solvation generally reflects specific solvent effects, careful selection of a probe solute allows for extrapolation regarding solvent–solute interaction for a species of interest (e.g., reactant, intermediate, catalyst) on the basis of the "surrogate's" behavior in the same mixed solvent system.

Using this approach, Fletcher and Pandey have studied the preferential solvation of the fluorescent probes pyrene and PyCHO dissolved in [bmim][PF_6]+water [75] and [bmim][PF_6]+ethanol [76] binary mixtures. Following from Eq. (1), Acree and coworkers have shown that in the absence of preferential solvation the observed pyrene I_1/I_3 intensity ratio for a binary solution of components A and B should become [74]

$$I_1/I_3 = \left[X_A I_{1,A} + (1 - X_A) I_{1,B}\right] / \left[X_A I_{3,A} + (1 - X_A) I_{3,B}\right] \tag{2}$$

where $I_{1,i}$ and $I_{3,i}$ are the experimental values for the pyrene band intensities in the pure solvents. Fletcher and Pandey observed that I_1/I_3 for pyrene in [bmim][PF_6] was unaffected by the water content even for the near-saturation value of 2.1 wt % (25 mol %) [75]. While this may seem surprising at first, one needs to consider that I_1/I_3 is related to ε and the refractive index, n, by the dielectric cross term [$f(\varepsilon,n^2)$]. More will be said about this later. At this point, it suffices to merely point out that since the dielectric constant of [bmim][PF_6] is only slightly lower than that of water, the magnitude of the total change in I_1/I_3 can be expected to be quite small. That is, Eq. (2) predicts that I_1/I_3 should only increase from 1.84 to 1.88 in going from anhydrous [bmim][PF_6] to [bmim][PF_6] containing 2.1 wt % water. Instead, the authors found that I_1/I_3 remains inexorably fixed across this range. The poor aqueous solubility of pyrene limits the precision with which I_1/I_3 can be measured in water, obviating a fully quantitative treatment. Still, there is clear evidence for preferential solvation of pyrene by [bmim][PF_6] ions. In line with these results, the Kamlet–Taft solvent dipolarity/polarizability, π^*, was also found to be uninfluenced by the water content in [bmim][PF_6] [77].

While pyrene was completely unresponsive to the addition of water to the [bmim][PF_6] phase, this was certainly not the case for PyCHO [75]. Instead, the PyCHO emission maximum increased monotonically from 425 to 443 nm as water was incrementally added to [bmim][PF_6] over a 0.0–2.1 wt % range. Using experimental emission maxima (R, R_A, R_B, expressed in cm^{-1}) and solving Eq. (1) for X_A allows the apparent solvation sphere composition to be determined as a function of the mole fraction of water in the bulk. The results of this exercise yield local water mole fractions of 0.10, 0.22, 0.29 and 0.36 for bulk mole fractions of 0.03, 0.10, 0.18 and 0.25. These results advance the notion that PyCHO experiences an environment enriched in water, particularly at lower mole fractions of water in the mixture. Hydrogen-bonding between water molecules and the aldehyde functionality on PyCHO likely plays a key role in this behavior. In addition, the overall reduction in viscosity induced by the addition of water may permit solvent relaxation to proceed to a greater extent with an accompanying red shift. Disentangling the relative contributions of these effects is not possible without detailed knowledge regarding the solvation dynamics of this system. Regardless, a limit of detection for water in this ionic liquid below 0.1 wt % was estimated from these results.

Another co-solvent with potential for modifying ionic liquid phases in a controlled fashion is ethanol. While [hmim][PF_6] and [omim][PF_6] are completely miscible with ethanol, the solubility limit of ethanol in [bmim][PF_6] is about 10 wt % at 25 °C. In recent partitioning studies, Rogers and coworkers observed large regions of complete miscibility in the three-component water–ethanol–[bmim][PF_6] system [78]. For this system, aqueous ethanol containing a 0.5–0.9 ethanol mole fraction was found to be totally miscible with [bmim][PF_6]. With important implications in the design of tunable green separations, this ternary system has been the subject of recent scrutiny [78–80].

Results of solvatochromic probe studies on the [bmim][PF_6]+ethanol system echo those from the [bmim][PF_6]+water mixture discussed above [76]. Again, I_1/I_3 does not change upon co-solvent addition, indicating that pyrene remains selectively solvated by [bmim][PF_6]. At a level of 40 mol % ethanol

in [bmim][PF_6], the I_1/I_3 value predicted from Eq. (2) is 1.65. However, the measured value is not appreciably different from the value in ethanol-free [bmim][PF_6], i.e., 1.88 versus 1.84 [56]. The reverse trend is observed for PyCHO which again has a strong affinity for the protic solvent component of the mixture (i.e., ethanol). As examples, ethanol mole fractions of 0.01 and 0.40 in the binary mixture resulted in *apparent* local ethanol mole fractions of 0.04 and 0.69, respectively, around PyCHO.

A third study by Fletcher and Pandey focused on the ternary [bmim][PF_6]+water+ethanol mixture [80]. In order to investigate this system it was necessary to recast Eqs. (1) and (2) to reflect an additional component. For example, the predicted pyrene I_1/I_3 ratio in a ternary solvent, assuming ideal solvent mixing is

$$I_1/I_3 = \left[X_A I_{1,A} + X_B I_{1,B} + X_C I_{1,C}\right] / \left[X_A I_{3,A} + X_B I_{3,B} + X_C I_{3,C}\right] \quad (3)$$

In the upper panel of Figure 4 are shown experimental pyrene I_1/I_3 results for a 0.55 mole fraction of ethanol in water as a function of the total mole fraction of added [bmim][PF_6]. The solid curve denotes the ideal behavior using Eq. (3). Differences in the observed minus predicted responses for several initial ethanol mole fractions are provided in the lower panel. It is important to note that all compositions fall within the monophasic region of the ternary phase diagram [78, 79]. Several features of these results bear specific mention. First, the experimental I_1/I_3 values are significantly higher than predicted across all compositions of the ternary system irrespective of the initial ethanol mole fraction in the aqueous ethanol. The negative deviation for a zero mole fraction of [bmim][PF_6] simply reflects the nonideality of aqueous ethanol [2]. So, despite the greater complexity of this system compared with the [bmim][PF_6]+water and [bmim][PF_6]+ethanol mixtures already discussed, the song remains the same. Again, pyrene is ostensibly sequestered within a [bmim][PF_6] enriched environment with respect to the bulk. In fact, for a [bmim][PF_6] mole fraction of 0.25 or greater these results are consistent with pyrene being solvated almost exclusively by [bmim][PF_6].

The corresponding PyCHO results are summarized in Figure 5. As illustrated in the top portion of the figure, the PyCHO emission energy remains fairly constant up to 35 mol % [bmim][PF_6]. In particular, the emission energy is akin to that of PyCHO in neat ethanol (ca. 22.3 kK) [56], suggesting marked preferential solvation by ethanol both in aqueous ethanol and upon addition of [bmim][PF_6]. For mole fractions of [bmim][PF_6] between 0.0 and 0.15 there is a large positive departure from molar additive behavior the extent of which decreases with higher initial ethanol mole fraction. A smaller and negative deviation for higher

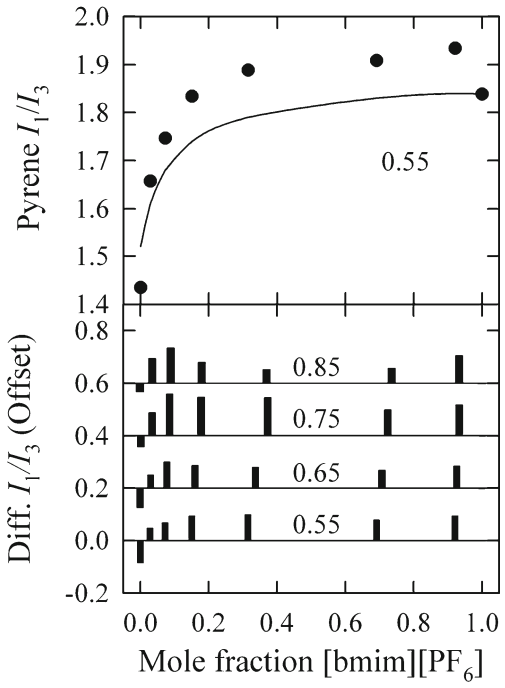

Fig. 4 Experimental pyrene I_1/I_3 values for a binary ethanol+water mixture (0.55 mole fraction ethanol) upon addition of [bmim][PF_6] as a third component compared with the ideal mole fraction additive curve (*upper*) and the excess polarities (observed minus ideal) at initial ethanol mole fractions of 0.55, 0.65, 0.75, and 0.85 (*lower*). Adapted from Reference 80

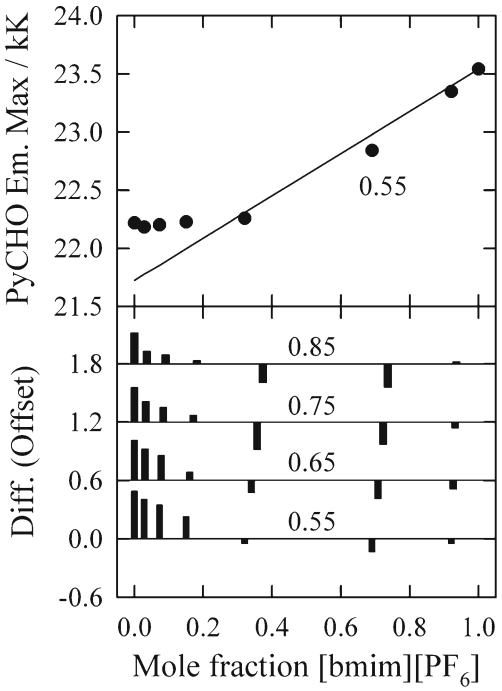

Fig. 5 Experimental PyCHO emission energies for a binary mixture of ethanol+water (0.55 mole fraction ethanol) as [bmim][PF_6] is added compared with the ideal curve (*upper*) and the emissive energy deviation from ideal mixing at initial ethanol mole fractions of 0.55, 0.65, 0.75, and 0.85 (*lower*); kK=1000 cm^{-1}. Adapted from Reference 80

[bmim][PF_6] mole fractions is also congruous with less pronounced preferential solvation by ethanol.

In other studies on using fluorescence to investigate cosolvent-modified ionic liquid based systems, the Samanta group used steady-state and time-resolved fluorescence behavior of coumarin 153 to study mixtures of [bmim][PF_6] with toluene and 1,4-dioxane [81]. Interestingly again, cosolvents appeared to have no significant effect on the steady-state fluorescence spectrum of the probe in this ionic liquid. The shift toward higher energy of the time-zero spectrum of the probe with gradual addition of the nonpolar solvent suggested that the probe experienced a more nonpolar environment at the early stage of the dynamics in mixed solvents. Further, this blue shift resulted in a larger Stokes shift of the time-dependent spectra due to solvent relaxation in mixed solvents. The authors compared the two systems and concluded that while a small amount of toluene could significantly affect the dynamics, a larger amount of dioxane was required to bring about the same effect. This was explained in terms of favorable interactions between toluene and the imidazolium ring system leading to a more effective solubilization of toluene in the cybotactic region of the probe. The same group also studied the excited-state proton transfer (ESPT) reaction of 7-hydroxyquinoline (7-HQ) in two ionic liquids mediated by methanol using steady-state and time-resolved fluorescence measurements [82]. While no ESPT was observed in neat ionic liquids, characteristic tautomer fluorescence of 7-HQ was observed in the presence of 0.5–4.1 M methanol. The rise time of the tautomer fluorescence was used to suggest the proton transfer in 7-HQ was an excited-state phenomenon that required considerable solvent reorganization prior to the relay of proton from the hydroxyl group to the distant ring nitrogen atom through a suitably organized dimeric chain of methanol molecules. The decrease in the rise time of the tautomer fluorescence with increasing methanol was attributed to the change of viscosity of the medium upon methanol addition. These authors noted the clear influence of viscosity on the ESPT kinetics along with lack of any definite correlation between the bulk viscosity and the rise time. A microheterogeneous nature of the media that does not allow assessment of the microviscosity around 7-HQ from the bulk viscosity was suggested to be the reason. The probe coumarin 153 was used by the Margulis group to investigate the effect of water on the dynamics of the ionic liquid [hmim][PF_6] by assessing the changes in the fluorescence behavior of the probe dissolved in the system [83]. Based on the outcomes, the authors suggested that water was closely associated with the anions and that its presence enhanced both the translational and rotational dynamics of the ionic liquid. They also reported that the fluorescence spectrum of the probe was red-shifted because of the presence of water. It was concluded that the interconversion between environments still occurred on a long time scale compared with the fluorescence lifetime of the probe. As an important outcome, emission from the probe was reported to be excitation wavelength dependent in both neat ionic liquid and (ionic liquid+water) mixtures.

Pandey and coworkers, anticipating the enormous potential of ionic liquid mixtures of polyethylene glycol (PEG), used three fluorescence probes, pyrene, PyCHO, and 1,3-bis-(1-pyrenyl) propane (BPP), to characterize properties of mixtures of PEG with [bmim][PF_6] [84]. All three probes demonstrated anomalous fluorescence behavior within the mixtures of [bmim][PF_6] with four different PEGs of average molecular weight 200, 400, 600, and 1500. Cybotactic region dipolarity of pyrene within the mixtures was observed by them to be higher than that expected from ideal additive behavior. PyCHO lowest energy fluorescence maxima showed values within the mixtures that were even higher than that in neat PEG, the component having the higher static dielectric constant of the two. Based on the fluorescence probe responses, the authors confirmed the "hyperpolarity" inherent to (PEG+[bmim][PF_6]) mixtures. The intramolecular excimer-to-monomer fluorescence intensity ratio of BPP indicated the microfluidity within the mixtures to be even lower than that within neat [bmim][PF_6], the component with the lowest microfluidity. The authors suggested an extensive hydrogen-bonded network involving terminal hydroxyls of PEGs and $[PF_6]^-$ as well as between ethoxy/hydroxyl oxygens of PEGs and the C2-H of $[bmim]^+$ to be the reason behind such behavior. Unusually altered physicochemical properties appear to be a key feature of the "hybrid green" (PEG+ionic liquid) system. In a separate investigation, the same group re-asserted these outcomes by investigating the dynamic viscosities of the mixtures of [bmim][PF_6] with PEGs of average molecular weight 200, 400, 570–630, and 950–1050 over the complete composition range at 10° intervals in the temperature range 10–90 °C [85]. The product of the monomer-to-excimer emission intensity ratio and the lifetime of the probe BPP was used as a reflection of the microviscosity of the mixtures. The microviscosity showed synergistic effects in all four ([bmim][PF_6]+PEG) mixtures. The authors noted the contribution of H-bonding to the microviscosity reported by BPP to be more than the contributions of Coulombic and van der Waals interactions. In subsequent studies, this group investigated the temperature-dependent behavior of the probes pyrene and PyCHO within water mixtures with the ionic liquid [bmim][BF_4] [86]. Surprisingly, the temperature dependent pyrene fluorescence behavior showed no clear-cut trend within aqueous mixtures of [bmim][BF_4]; PyCHO also appeared insensitive toward temperature changes. In a recent investigation, Pandey and coworkers have demonstrated that mixtures of [bmim][PF_6] and 2,2,2-trifluoroethanol (TFE) also display the intriguing phenomenon of

hyperpolarity based partly on the responses of fluorescent probes capable of engaging in hydrogen bonds, 2-(p-toluidino)naphthalene-6-sulfonate (TNS) and 6-propionyl-2-(dimethylamino)naphthalene (PRODAN) [87]. The authors reported the choice of ionic liquid anion to be essential as hyperpolarity was not observed for mixtures of TFE with ionic liquids containing anions other than $[PF_6]^-$. The complex solute−solvent and solvent−solvent interactions present in the [bmim][PF_6]+TFE mixture were elucidated using infrared absorbance, dynamic viscometry, and density measurements in this report. The results were discussed by the authors in terms of Coulombic interactions, disruption of TFE multimers, formation of hyperanion preference aggregates, and "free" $[bmim]^+$.

Ali et al., while investigating the properties of aqueous mixtures of the ionic liquid [bmim][BF_4], noticed unusual fluorescein prototropism within these mixtures [88]. Specifically, fluorescence emission of the cationic form of fluorescein was observed from dilute aqueous acidic solution in the presence of this ionic liquid, which was otherwise observed only from aqueous solutions of very high acidity. The observation was rationalized based on the [bmim][BF_4]-rich solvation sphere of fluorescein. In aqueous fluorescein solutions of moderate acidity, the fluorescence emission could only be observed from the neutral and/or the monoanionic species because of the extremely fast deprotonation of the cationic species in the excited state. At higher [bmim][BF_4] concentrations, the solvation sphere (especially the cybotactic region) of the excited state became rich in [bmim][BF_4] and afforded fewer water molecules, thus hindering the rapid deprotonation. The ionic liquid [bmim][BF_4], unlike water which played the role of proton acceptor in this scenario, was unable to accept a proton from the cationic species, thus restricting its conversion to the neutral and/or monoanionic forms.

Binary Ionic Liquid Mixtures

The most common approach toward optimizing ionic liquid media for a given application involves design of the ionic liquid itself. For instance, appropriate functional engineering of the [X-mim][Tf_2N] family has been shown to result in a substantial increase in the observed range of polarity [17]. Use of co-solvents adds a further dimension of control over the properties of ionic liquid-based solvent systems. Another option that has gone virtually unexplored to date is the use of ionic liquid mixtures.

The first investigation of this kind was reported by the Pandey group [89]. In this study, the binary ionic liquid mixtures [bmim][Tf_2N]+[bmim][PF_6], [emim][Tf_2N]+[bmim][PF_6], and [emim][Tf_2N]+[bmim][Tf_2N] were explored using fluorescence spectroscopic approaches developed in earlier work by the group [75, 76, 80]. Figure 6 summarizes the effects of binary composition on pyrene I_1/I_3 values for these three mixtures. In all cases, I_1/I_3 values were higher than predicted, suggesting an increased local dielectric relative to ideal mixing although the mixed cation [emim][Tf_2N]+[bmim][Tf_2N] system behaved most ideally. In this case, the authors invoked minor packing efficiency effects to explain the slight deviation from the expected response. Much more pronounced deviation from the theoretical curve was seen for [bmim][Tf_2N]+[bmim][PF_6] (the mixture shown in the upper portion of Figure 6) and the most nonideal response was observed for [emim][Tf_2N]+[bmim][PF_6]. These results were postulated to result from competitive anion coordination effects altering the relative anion–pyrene interaction strength or pyrene locating in a microscopically heterogeneous cavity as a result of such interactions. In this regard, it is well known that the negative charge is localized across the S–N–S moiety in $[Tf_2N]^-$ resulting in a more strongly coordinating anion than $[PF_6]^-$.

Results of PyCHO based studies of these same binary ionic liquid mixtures are provided in Figure 7. In contrast with earlier studies of binary [bmim][PF_6]+water [75] or ethanol [76] mixtures, large changes are not to be expected since the PyCHO emission maxima in all three ionic liquids falls in the 423–427 nm range. Indeed, this is the case. Given the experimental uncertainty, no clear-cut preferential solvation is suggested.

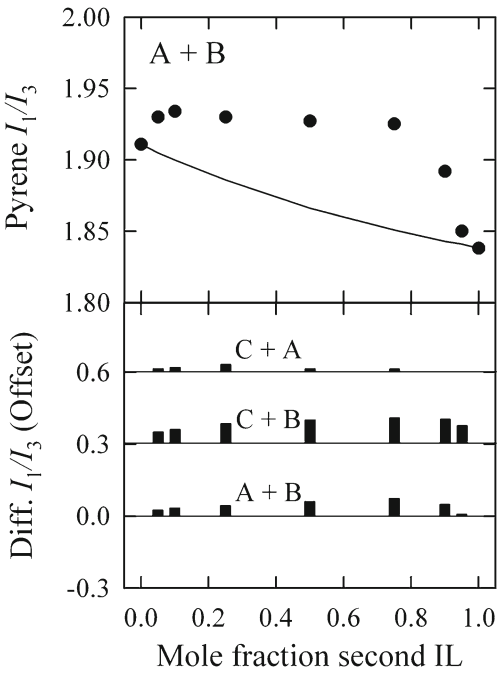

Fig. 6 Experimental pyrene I_1/I_3 values for the binary ionic liquid mixture A+B. The solid curve denotes ideal mixing for this mixture as predicted by Eq. (2) (*upper*). The excess polarities for the mixtures: A+B, C+B, and C+A where A=[bmim][Tf_2N], B=[bmim][PF_6], and C=[emim][Tf_2N] (lower). The second component in each pairing has a lower polarity on the basis of I_1/I_3 values. Adapted from Reference 89

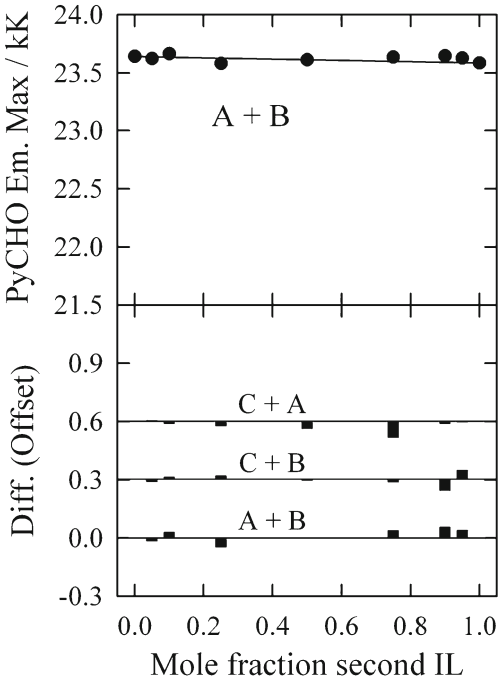

Fig. 7 Experimental PyCHO emission energies for the binary ionic liquid mixture A+B compared with the behavior predicted by Eq. (1) (*upper*). The emission energy differences (obs minus calc) for binary mixtures A+B, C+B, and C+A. The identity of the ionic liquids is the same as for Figure 6 (*lower*). Adapted from Reference 89

Ionic Liquids Plus CO_2

VOCs are common industrial solvents with worldwide usage exceeding five billion US dollars each year. Unfortunately, the continued use of VOCs presents many serious drawbacks. Among these are various factors such as disposal and recycling costs, pollution prevention, worker safety issues, and tight usage regulations. Consequently, there is substantial economic, environmental, political and social pressure to develop environmentally benign alternatives to replace VOCs [90–93].

Among the pedigree of approaches developed, supercritical fluids (SCFs) [94–98] and ionic liquids [99–101] have each emerged as viable solvents to replace undesirable VOCs. A major challenge that exists in the use of ionic liquids is that it is often difficult to separate products from reactants, catalysts, or solvent. The marriage of these two media offers a possible answer with supercritical CO_2 ($scCO_2$, T_c=31.1 °C, P_c=73.8 bar) being the most popular SCF under exploration [102–105]. Investigations in this area have demonstrated that while $scCO_2$ is highly soluble in certain ionic liquids, the reverse is not true. This fortunate phase behavior makes possible the recovery of solutes from ionic liquids while completely eliminating the problem of cross-contamination encountered in liquid/liquid extraction. For example, Blanchard et al. [102] showed the near quantitative extraction of naphthalene from [bmim][PF_6] using $scCO_2$ with no loss of the ionic liquid.

A notable study by Kazarian et al. [103] used *in situ* ATR (attenuated total reflectance)-FTIR to gain insight into the molecular state of CO_2 dissolved at high pressure in the ionic liquids [bmim][BF_4] and [bmim][PF_6]. In this work, the degree of the splitting of the bending mode (ν_2) of dissolved CO_2 suggested that $[BF_4]^-$ was a stronger Lewis base than $[PF_6]^-$ toward CO_2. In addition, based on the intensity of the ν_3 antisymmetric stretching band, the authors found that the uptake of CO_2 by [bmim][PF_6] at 68 bar and 40 °C was approximately 0.6 mole fraction (2.0 M). The estimated solubility of CO_2 in [bmim][BF_4] was ca. 40 % less, an amount consistent with the lower swelling of this ionic liquid as a result of CO_2 uptake.

The Bright [104] and Eckert [105] groups have each reported on the microscopic solvent properties of [bmim][PF_6]+CO_2 mixtures using different fluorescent solvatochromic probes. In the first study, the authors used pyrene and PRODAN to probe the local polarity/polarizability surrounding these fluorescent solutes while the later study used DCVJ for this purpose.

Figure 8(a) presents pyrene I_1/I_3 values as a function of $f(\varepsilon,n^2)$ for a number of common solvents. The pyrene I_1/I_3 band ratio is related to ε and n by the dielectric cross term, $f(\varepsilon,n^2)$ as given by the following expressions [57, 104]

$$I_1/I_3 = A + B \cdot f\left(\varepsilon, n^2\right) \tag{4}$$

$$f\left(\varepsilon, n^2\right) = \left[(\varepsilon - 1)/(2\varepsilon + 1)\right] \cdot \left[\left(n^2 - 1\right)/\left(2n^2 + 1\right)\right] \tag{5}$$

These results suggest that the cybotactic region surrounding pyrene in [bmim][PF_6] has a dipolarity akin to DMSO. In Figure 8(b), the same results are plotted as a function of ε. Although the correlation is poorer, contrasting the PyCHO results discussed in a previous section, the I_1/I_3 value for [bmim][PF_6] is consistent with a ε of 40 or higher. A dielectric constant of this magnitude is not unreasonable given recent results from the Eckert lab [105]. Using the charge-transfer probe DCVJ whose emission maximum (in nm) is a linear function of ε, Eckert and co-workers estimated that ε for [bmim][PF_6]/CO_2 mixtures increases from about 41 to 44 with increased equilibrium CO_2 pressure from 0 to 200 bar at 35 °C. The insignificant effect of [bmim][PF_6] taking up considerable amounts of CO_2 at these higher pressures [103] is indicative of preferential solvation of DCVJ by [bmim][PF_6] solvent ions. Similarly, as CO_2 was added to pure [bmim][PF_6] from 0 to 130 bar at 35 °C, the decrease in pyrene I_1/I_3 was also notably small (from 2.02 to 1.92) [104]. Consider that, based on pyrene I_1/I_3

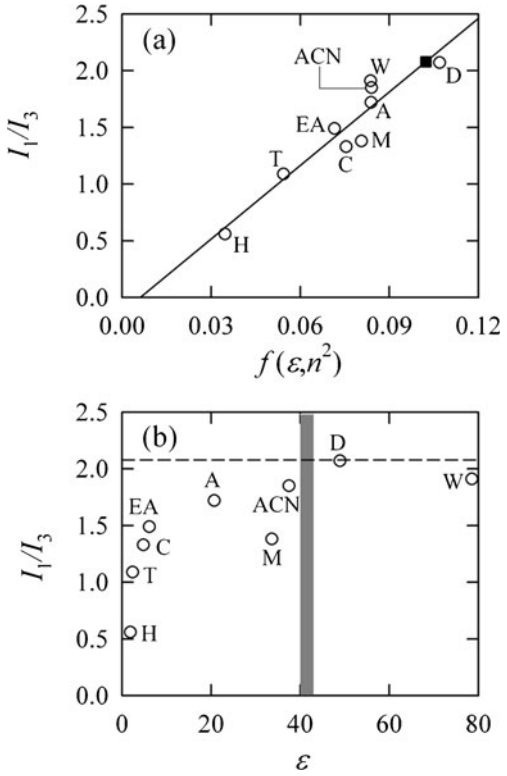

Fig. 8 Correlation between pyrene I_1/I_3 values and the solvent dielectric cross term (**a**) and static dielectric constant (**b**) for a number of conventional organic solvents at 20 °C. The interpolated I_1/I_3 value for [bmim][PF_6] is shown as the filled symbol ■ in (**a**). The dashed horizontal line in (**b**) denotes the measured I_1/I_3 value in [bmim][PF_6] and the shaded region shows the estimated ε for [bmim][PF_6] taken from Reference 105. The identities of the solvents are as follows: *n*-hexane (H); toluene (T); ethyl acetate (EA); chloroform (C); methanol (M); acetone (A); acetonitrile (ACN); water (W); dimethyl sulfoxide (D)

values in pure $scCO_2$, ideal mixing should result in an I_1/I_3 below 1.40 at higher CO_2 densities. These results argue that the intermolecular interactions between pyrene and [bmim][PF_6] are mediated by the addition of CO_2, but not significantly so. In fact, this minimal decline in I_1/I_3 at high CO_2 pressure implies a local enhancement of ionic liquid composition around the pyrene indicator. The ability to maintain solvent strength even at high loadings of CO_2 is an important feature of the [bmim][PF_6]/CO_2 system.

Like pyrene, the Stokes shift (*SS*, in cm^{-1}) for PRODAN also depends on the solvent's ε and *n* through the Lippert–Mataga expression [57, 104]

$$SS = (\mu_E - \mu_G)^2(2\Delta f)/(hca^3) + \text{constant} \qquad (6)$$

In this expression, μ_E and μ_G are PRODAN's excited-state and ground-state dipole moments, respectively, *h* is Planck's constant, *c* is the speed of light, *a* is radius of the cavity swept out by PRODAN, and Δf, the orientational polarizability, is given by

$$\Delta f = [(\varepsilon - 1)/(2\varepsilon + 1)] - [(n^2 - 1)/(2n^2 + 1)] \qquad (7)$$

A Lippert plot for PRODAN dissolved in a wide range of pure liquids (Figure 9) suggests that Δf for [bmim][PF_6] falls within the 0.20–0.26 range, consistent with a regional dipolarity between chloroform and DMF. To reconcile the apparent incongruity between the pyrene and PRODAN results in this study, the authors simultaneously solved Eqs. (5) and (7) for ε and *n* using the apparent $f(\varepsilon,n^2)$ and Δf values for [bmim][PF_6] indicated in Figures 8(a) and 9, respectively. This exercise yielded ε and *n* values of 11.4 and 1.52, respectively, when Δf was estimated from the entire solvent set shown in Figure 9. When the protic solvents were removed from the fit in Figure 9, however, the shifted Δf resulted in ε and *n* values of 30.0 and 1.46. This value for ε agrees reasonably well with the DCVJ-determined ε reported by Eckert and co-workers [105]. Likewise, Bonhôte et al. [48] reported a mean *n* of 1.43 for a variety of [bmim]-based ionic liquids. In retrospect, Δf (and concomitantly ε) may have been underestimated as a result of incomplete solvent relaxation on the timescale of the emission process. Frequency-domain phase-modulation results shown in Figure 10 provide unequivocal evidence for nanosecond dipolar relaxation surrounding PRODAN in [bmim][PF_6] [104]. In addition to the fluorescence lifetime increasing with emission wavelength, at high frequencies the phase angle for PRODAN red-edge emission collected with a 515 nm longpass (LP) filter clearly exceeds 90° (shown by the arrow in Figure 10). This is indicative of an

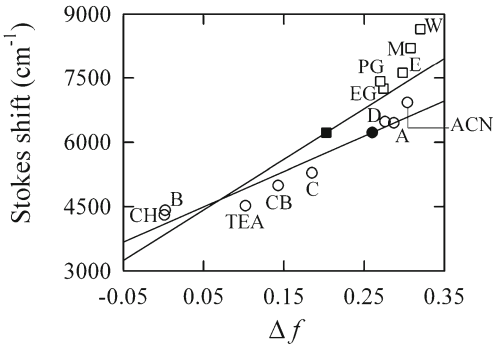

Fig. 9 Lippert plot for PRODAN dissolved in a number of aprotic (○) and protic (□) solvents at 20 °C. The experimental Stokes shift for PRODAN in [bmim][PF_6] (6225 cm^{-1}) falls on the linear regression line for all solvents at the position denoted by ■. The corresponding orientational polarizability determined from only the aprotic solvents is indicated by ●. The identities of the solvents are as follows: cyclohexane (CH); benzene (B); triethylamine (TEA); chlorobenzene (CB); chloroform (C); *N*,*N*-dimethylformamide (D); acetone (A); acetonitrile (ACN); ethylene glycol (EG); propylene glycol (PG); ethanol (E); methanol (M); water (W)

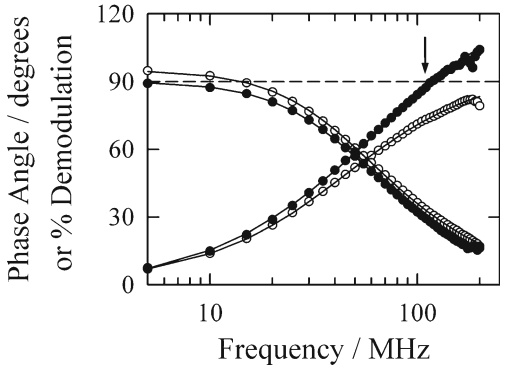

Fig. 10 Multifrequency phase–modulation data for PRODAN in [bmim][PF_6] at 20 °C monitored over the entire emission profile (400 nm LP filter, ○) or the emission red edge (515 nm LP, ●). Solid traces represent best fits to a triple-exponential decay model and the dashed horizontal line indicates a phase angle of 90°

excited-state reaction and is wholly consistent with dipolar solvent relaxation.

Bright and co-workers also reported on nanosecond fluorescence anisotropy measurements of the rotational mobility of the neutral, nonpolar fluorescent probe *N*,*N*′-*bis*(2,5-di-*tert*-butylphenyl)-3,4,9,10-perylenedicarboximide (BTBP) in [bmim][PF_6] as functions of temperature and CO_2 [104]. Because BTBP is a spherical rotor [106–108], its rotational reorientation dynamics are well described by a single rotational correlation time, θ, that depends on the solvent viscosity as given by the Debye–Stokes–Einstein hydrodynamic model [57]

$$\theta = \eta V/RT \tag{8}$$

where V is the volume of the reorienting entity and R and T represent the gas constant and Kelvin temperature, respectively. The rotational correlation time is related to the rotational diffusion coefficient by $\theta=(6D)^{-1}$.

Figure 11(a) summarizes the effects of temperature (25–60 °C) on the BTBP rotational correlation time in neat [bmim][PF_6]. The increased BTBP mobility with increasing temperature follows Arrhenius behavior and, in fact, the activation energy for rotational reorientation (E_r=38.9± 1.9 kJ mol^{-1}) was found to be statistically equivalent to the activation energy for viscous flow (E_η=38.4±0.9 kJ mol^{-1}) over the temperature range 25–70 °C as shown in Figure 11(b) [104]. These results signify that the BTBP rotational dynamics are correlated entirely with the [bmim][PF_6] dynamics.

As illustrated in Figure 12(a), addition of CO_2 (0–138 bar) to [bmim][PF_6] results in a nearly seven-fold decrease in θ. The CO_2-dependent [bmim][PF_6] microviscosity estimated using Eq. (8) under the assumption that solvent attachment does not occur (V≈733 $Å^3$ for unsolvated BTBP) [106, 107] is provided in Figure 12(b). These results are in remarkable agreement with later studies by Eckert and co-workers considering that these authors used a

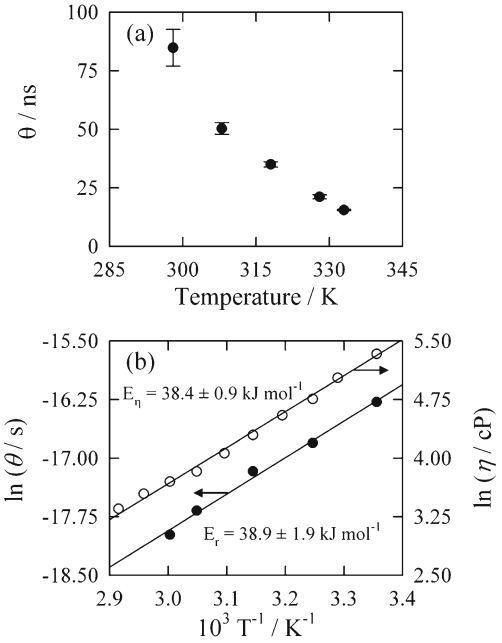

Fig. 11 (**a**) Effect of temperature on the rotational correlation time of BTBP dissolved in [bmim][PF_6]. (**b**) Arrhenius plots comparing E_η with E_r for BTBP in [bmim][PF_6]

different probe (DCVJ) to explore the [bmim][PF_6]/CO_2 system [105]. A molecular rotor, DCVJ, exhibits an exceptionally high and viscosity-dependent rate for internal conversion, on the order of 10^{11} s^{-1} [109–111]. Factors that resist the torsional relaxation of DCVJ, such as increased

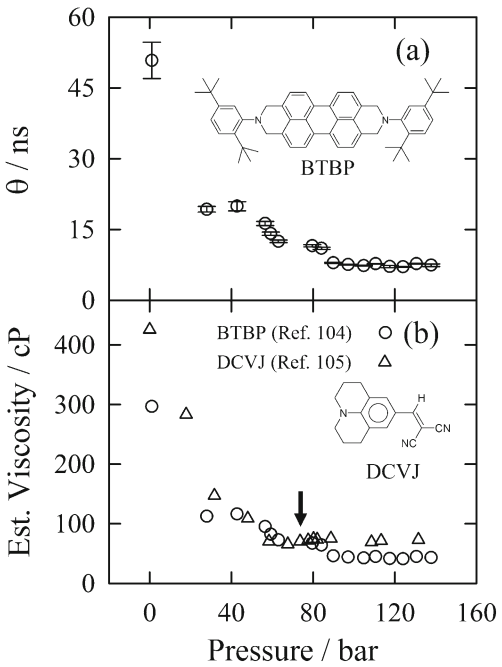

Fig. 12 Influence of CO_2 addition on (**a**) the BTBP rotational correlation time and (**b**) the estimated microviscosity surrounding BTBP and DCVJ in [bmim][PF_6] at 35 °C. The arrow in panel (**b**) marks the critical pressure (P_c) of CO_2

viscosity, lower the nonradiative decay rate, k_{nr}, manifesting in a higher fluorescence yield, Φ_f. Using the linear correlation between the natural logarithm of DCVJ fluorescence intensity (ln F) and ln η, these authors also determined the apparent viscosity of [bmim][PF_6] upon addition of CO_2. Results from the Bright [104] and Eckert [105] labs, compared directly in Figure 12(b), indicate 6.8 and 6.5-fold overall reductions in η, respectively, with a plateau occurring near P_c. The chief discrepancy in these two studies, the different estimated viscosities of pure [bmim][PF_6], was attributed to the presence of differing levels of impurity in the ionic liquids, particularly water and halides. Nevertheless, it is apparent that, even at moderate pressures, CO_2 is capable of acting as an effective diluent or "lubricant", with the potential for promoting mass transport and facilitating separations within ionic liquid phases.

In an investigation of analytical interest, it is shown that uranyl ions $[UO_2]_2^+$ in aqueous nitric acid can be extracted into supercritical CO_2 by using an imidazolium-based ionic liquid with tributylphosphate (TBP) as the complexing agent [112]. While the initial transfer of uranium from the ionic liquid to the supercritical fluid phase was monitored by uv-vis spectroscopy using a high-pressure fiber-optic cell, the extraction process was monitored by fluorescence spectroscopy along with neutron activation analysis. This fluorescence based methodology was projected to have potential applications in the field of nuclear waste management for extracting other actinides. Kimura et al. investigated the effects of dissolved CO_2 in ionic liquids [bmim][PF_6] and [bmim][Tf_2N], respectively, by time resolved fluorescence spectroscopy using the probe coumarin 153 [113]. The solvation dynamics within the mixture showed an ultrafast response less than 1 pico-second and a slower response extended to a half of nano-second under ambient condition. It was observed that upon increasing the CO_2 pressure, the slower component became faster with no apparent change in the faster component. The authors compared the effect of CO_2 on average solvation time with that on the translational diffusion of the fluorescence probe dissolved in the (ionic liquid+CO_2) mixture.

Different fluorescence chemosensors have been used to detect dissolved CO_2 within various ionic liquid based systems. In one of the early investigations, the authors described the characterization of a new optical CO_2 sensor based on the change in the fluorescence signal intensity of 8-hydroxypyrene-1,3,6-trisulfonic acid trisodium salt (HPTS) in the ionic liquids [bmim][BF_4] and [bmim][Br] [114]. The authors noted the important observation that the solubility of CO_2 in water-miscible ionic liquids was ~10 to 20 times that in conventional solvents, polymer matrixes, or water. The response of the fluorescent HPTS sensor to gaseous and dissolved CO_2 in the above ionic liquids was evaluated by the authors, which showed that the luminescence intensity of HPTS at 519 and 521 nm decreased with increasing concentrations of CO_2 by 90 % and 75 % in the two ionic liquids, respectively. The acceptable response times of the sensing reagent was shown to be in the range 1–2 min for switching from nitrogen to CO_2, and 7–10 min for switching from CO_2 to nitrogen. The signal changes were found to be fully reversible and no significant hysteresis was reported by the authors. The excellent stability of the fluorescence probe HPTS in the ionic liquids when stored in the ambient air of the laboratory was emphasized based on no significant drift observed in signal intensity even after 7 months. The Wolfbeis group developed optical CO_2 sensors based on emulsion of ionic liquids in a silicone matrix [115]. Their quantitative fluorometric sensor also made use of HPTS. The authors showed that the response of their fluorometric sensors to CO_2 could easily be linearized which made calibration of the sensors very simple. Authors also demonstrated use of a reference inert fluorescent dye (4-dicyanomethylene-2-methyl-6-(4-(dimethylamino)styryl)-4 H-pyran) which could be added for ratiometric measurements. The authors proposed that their sensors could find applications in biotechnology, environmental monitoring, and food-packaging technology. In a recent investigation, a new optical sensor for dissolved CO_2 based on the spectrofluorimetric signal changes of the fluorescent phenyl-linked carbazole oxazolones in ionic liquids was proposed [116]. The response of this fluorescence probe-based chemosensor to both gaseous and dissolved CO_2 was tested in ethyl-cellulose- and imidazolium-based ionic liquids. For dissolved CO_2, the detection limit was found to be 5×10^{-7} M. The authors noticed that when embedded in ionic liquids, their fluorescence chemosensor exhibited excitation wavelengths beyond 465 nm, extinction coefficients around 185,000 cm^{-1} M^{-1}, and Stokes shifts extending to 56 nm. The ionic liquid [emim][BF_4] provided longer storage time and a highly stable microenvironment for the fluorescent probe due to the buffering effect. It was noted by the authors that their dissolved CO_2 sensor based on dye-doped ionic liquid did not need extra protection from the ambient air of the laboratory.

Ionic Liquids Plus Surfactants

A related area which has also received considerable attention is the use of conventional surfactants to form micelles or other self-assemblies within an ionic liquid continuous phase [117–119]. In an early report, Anderson et al. [117] investigated the effects of adding the traditional surfactants Brij-700, Brij-35, dioctyl sulfosuccinate (AOT), caprylyl sulfobetaine, and sodium dodecyl sulfate (SDS) to the ionic liquids [bmim][Cl] and [bmim][PF_6]. Light and neutron scattering techniques, surface tension measurements, and inverse gas chromatography were used to characterize the

aggregation occurring in these mixtures and were generally consistent with micelle formation or at least amphiphilic association of some kind in these ionic liquids. We note that, for a given surfactant, the critical aggregate concentration (CAC) was generally between one and two orders-of-magnitude higher than the corresponding value in water. In another study, Fletcher and Pandey utilized pyrene as a probe solute to study the impact of charged versus uncharged surfactants on the cybotactic region polarity in [emim][Tf_2N] [118]. Pursuant to these studies, addition of the well-studied cationic surfactant cetyltrimethylammonium bromide (CTAB) produced no change in the observed pyrene I_1/I_3 ratio up to its solubility limit in [emim][Tf_2N] (≈0.25 M) while SDS apparently had negligible solubility in this ionic liquid. Several nonionic surfactants (Brij-35, Brij-700, Tween-20, and Triton X-100) on the other hand appeared to aggregate in a concentration-dependent manner with a sharp discontinuity in I_1/I_3 denoting the onset of micellization. Again, the CACs estimated for the nonionic surfactants were far larger than that in water. Their results using the fluorescent microviscosity probe BPP were consistent with spontaneous aggregate formation in the same concentration regime.

Of course, appropriately formulated ionic liquid type salts may function as surfactants themselves when added to water or other solvent systems including conventional ionic liquids [120–125]. For example, Merrigan et al. [120] showed that methyl or *n*-butyl imidazolium cations appended with long fluorous 'ponytails' were able to emulsify perfluorohexane into [hmim][PF_6]. In addition, long-chain surfactants based on 1-alkyl-3-methylimidazolium [121, 122] or *N*-alkyl-*N*-methylpyrrolidinium cations [123, 124] do indeed form micelles in water. Using 2-hydroxy Nile Red (HONR) as a fluorescent probe, Miskolczy et al. [121] studied the association in water of ionic liquids containing the *n*-octyl moiety either as part of the cation or anion. In this study, HONR exhibited bi-exponential fluorescence intensity decays with the fractional contribution of the longer-lived decay component having a sigmoidal dependence on the [bmim] [octylsufalte] concentration. The critical micelle concentration (CMC) determined from the sigmoidal inflection point (~31 mM) was in excellent agreement with the conductivity-based break points. Although [omim][Cl] produced an inhomogeneous solution of large aggregates, inclusion as a co-surfactant in a mixed micelle with SDS resulted in a significant diminution in the polarity experienced by HONR in the interfacial Stern layer. In similar fashion, the very low pyrene I_1/I_3 value for *N*-octadecyl-*N*-methylpyrrolidinium bromide at an aqueous concentration exceeding the CMC suggested a dipolarity akin to toluene [123]. Presumably, both of these results originate from a reduced penetration of water in the vicinity of the probe solute. Longer-chain ionic liquids may also self-assemble to form thermotropic liquid-crystalline mesophase ionic liquids [126], and lyotropic mesophases in concentrated aqueous solutions of [dmim]Br, an ionic liquid with a moderate chain length, have also been reported [127].

Over the past few years, the Pandey group has systematically investigated the changes in the properties of aqueous surfactant solution upon ionic liquid addition using various fluorescence probes [128–135]. They started their investigation with an aqueous surfactant solution formed by a nonionic surfactant Triton X-100 (TX-100) [128, 129]. Their first investigation was based on studying the effect of addition of the hydrophobic ionic liquid [bmim][PF_6] using fluorescence from pyrene, PyCHO, 2-(p-toluidino) naphthalene-6-sulfonate, and BPP along with that from the phenyl group inherent to the surfactant TX-100 [128]. The fluorescence probe response strongly suggested the partitioning of the ionic liquid into the micellar pseudo-phase. While statistically insignificant increases in critical micelle concentrations (CMC) and decreases in aggregation number (N_{agg}) of TX-100 micelles were reported as 2 % [bmim][PF_6] was added, use of up to 30 % [bmim][BF_4], a 'hydrophilic' ionic liquid, resulted in decreased N_{agg} and increased CMC indicating an overall unfavorable aggregation process [129]. Further, increase in the dipolarity and the microfluidity of the probe cybotactic region within the palisade layer of the micellar phase upon [bmim][BF_4] addition implied increased water penetration and the possibility of TX100-[bmim][BF_4] interactions. The effect of ionic liquid addition on aqueous anionic sodium dodecyl sulfate (SDS) was reported next by the authors [130, 134]. As revealed by the fluorescence probes' responses, addition of up to ~ 0.10 % [bmim][PF_6] resulted in a dramatic decrease in the CMC accompanied by an increase in the N_{agg} indicating micellar growth [130]. Significantly decreased microfluidity of the aqueous SDS upon addition of [bmim][PF_6] was indicated by the response of BPP, which suggested partitioning of the ionic liquid into the SDS micellar phase. The behavior of pyrene, PyCHO, and 2-(p-toluidino)naphthalene-6-sulfonate confirmed the interaction and possible complexation between the ionic liquid and the anionic micellar surface. Presence of strong electrostatic attractions between $[bmim]^+$ and the anionic micellar surface was proposed to be the most dominant reason for these observations. While the changes in the properties of aqueous SDS solution were observed to be similar as 2 % hydrophilic [bmim][BF_4] was added [131], further increase in [bmim][BF_4] concentration to 30 % resulted in an increase in CMC and a decrease in N_{agg}. The role of an ionic liquid in altering the properties of aqueous SDS in the range 2 %<[bmim][BF_4]≤30 % was found to be similar to those of polar co-solvents. The concentration-dependent dual role of the ionic liquid [bmim][BF_4] in altering physicochemical properties of aqueous SDS was demonstrated by the authors. The

addition of ionic liquid to the aqueous solution of CTAB, a cationic surfactant, was carried out next by this group [132]. In this context, the effects of [hmim]Br addition were compared with those of a co-surfactant *n*-hexyltrimethylammonium bromide (HeTAB). The fluorescence probe responses revealed the changes in most of the physicochemical properties to be significantly more dramatic in the case of [hmim]Br addition. The fact that, between the two, only [hmim]Br showed co-solvent type behavior at high concentrations was evoked to explain the differences in the behavior of the two additives. Both [hmim]Br and HeTAB showed electrolytic as well as cosurfactant-type behavior when present at low concentrations, whereas at high concentrations, while HeTAB still acted as a cosurfactant forming mixed micelles with CTAB, [hmim]Br behaved partly as a cosolvent toward altering the physicochemical properties of aqueous CTAB. Similar investigations on the zwitterionic surfactant *N*-dodecyl-*N*,*N*-dimethyl-3-ammonio-1-propanesulfonate (SB-12) solution using fluorescence probes also revealed that ionic liquids could alter the physicochemical properties of this aqueous surfactant solution in a unique manner [133, 134]. The extent to which these properties are altered was observed to be significantly more for [bmim][PF_6] as compared to that for [bmim][BF_4] [133]. The interaction between the ionic liquid anion and the cationic quaternary ammonium of SB-12 was proposed to be more efficient for [bmim][PF_6] due to the bigger size of $[PF_6]^-$. The important role of the ionic liquid anion in modifying properties of aqueous SB-12 was demonstrated. Based on all these studies, the authors concluded that the behavior of an ionic liquid within aqueous micellar solutions was governed by its unique property to act both as an electrolyte and a cosolvent [135]. The possibility of formation of oil-in-water microemulsions in which the ionic liquid acted as the "oil" phase was also presented. Based on the observation that the solubility of [bmim][PF_6] within aqueous nonionic and zwitterionic micellar solutions increased with increasing surfactant concentration, the formation of ionic liquid-in-water microemulsions was suggested.

Several research groups have used various time-resolved fluorescence based techniques to investigate the effect of the presence of ionic liquids in normal and reverse micelles and various microemulsions [136–144]. In this regard, major efforts come from the Bhattacharyya group [136, 137] and The Sarkar group [138–141]. The effect of an ionic liquid and water on the ultrafast ESPT of HPTS inside a microemulsion consisting of surfactant TX-100 in benzene and containing the ionic liquid [pmim][[BF_4] (p = pentyl) as the polar phase was studied by femtosecond up-conversion [136]. It was proposed that in the ionic liquid microemulsion, HPTS was bound to the TX-100 at the interface region and participated in ultrafast ESPT to the oxygen atoms of TX-100. It was further suggested that the added water preferentially got trapped around the palisade layer of the ionic liquid microemulsion and remained far from the HPTS both in the presence and absence of ionic liquid. In the other investigation, fluorescence resonance energy transfer (FRET) from coumarin 480 to rhodamine 6G was studied in the same ionic liquid microemulsion by picosecond and femtosecond emission spectroscopy [137]. It was suggested that the highly polar ionic liquid pool was probed where FRET was very fast due to the close proximity of the donor and the acceptor. Another ionic liquid, 1-methyl-1-propypyrrolidinium [Tf_2N] was used as the polar solvent to form non-aqueous reverse micelles (RMs) with benzene by the aid of the cationic surfactant BHDC [138] and the nonionic surfactant TX-100 [139]. The dynamics of solvent relaxation were studied in these systems using steady-state and time-resolved fluorescence spectroscopy using coumarin 153 and coumarin 480 fluorescence probes with variation in the ionic liquid content in the microemulsions. For both of the probes, it was observed that with an increasing amount of ionic liquid in the microemulsions, the relative contribution of the fast components increased and the slow components contribution decreased resulting in a decrease in average solvation time. Similar outcomes were observed when ionic liquid 1,1,1-trimethyl-1-propylammonium [Tf_2N] was substituted for polar water and formed microemulsions with cyclohexane by the aid of nonionic surfactant TX-100 [140]. The dynamics of solvent and rotational relaxation were investigated using steady-state and time-resolved fluorescence spectroscopy as a tool and coumarin 480 as a fluorescence probe. The size of the microemulsions increased with gradual addition of the ionic liquid leading to the faster collective motions of cation and anions of the ionic liquid, which contributed to faster solvent relaxation in microemulsions. The dynamics of solvent and rotational relaxation of coumarin 153 in the ionic liquid [bmim][PF_6] confined in Brij-35 micellar aggregates were investigated using steady-state and time-resolved fluorescence spectroscopy [141]. The authors observed slower dynamics in the presence of micellar aggregates as compared to the pure ionic liquids. However, it was revealed that the slowing down in the solvation time on going from neat ionic liquid to ionic liquid-confined micelles was much smaller compared to that on going from water to water-confined micellar aggregates. The increase in solvation and rotational time in micelles was attributed to the increase in the viscosity of the medium.

A perylenetetracarboxylic diimide (PDI) compound with an attached hydrophilic polyoxyethylene group at the imide *N* position was used to study the photoinduced electron and energy transfer between it and coumarin 153 in a ternary microemulsion with an ionic liquid (i.e., [bmim][PF_6]/TX-100/water) utilizing fluorescence spectroscopy [142]. The authors found that both PDI and coumarin 153 resided at the interface between the surfactant TX-100 and the ionic liquid

in the ternary microemulsions. Interestingly, while the absorption spectra suggested no interactions between coumarin 153 and PDI in the ground states, the fluorescence spectra revealed the presence of an efficient electron transfer and a less efficient energy transfer from coumarin 153 to PDI. Moreover, the electron transfer was observed to be much more efficient in microemulsions than in homogeneous conventional organic solvents due to the unique microenvironment of the microemulsion. The aqueous mixtures of an anionic surfactant, sodium dodecyl benzene sulfonate (SDBS), and, [bmim][BF_4], were shown to spontaneously separate into two immiscible aqueous phases: one surfactant-rich and the other ionic liquid-rich within a certain range of compositions [143]. This phase separation phenomenon was proposed to be likely due to the existence of micelle aggregates with quite large size as confirmed using steady-state fluorescence quenching measurements of pyrene fluorescence by the quencher benzophenone. Zhu and Jiang developed a method for the determination of iron (III) based on the fluorescence quenching of salicylfluorone (SAF) by iron(III), where it was shown that the fluorescence quenching could be increased in the mixture of [emim][ethylsulfate]+SDS [144]. The linear range of the calibration curve was found to be 0.2–1.1 $\mu g/mL^{-1}$ and the detection limit was estimated to be 8.3 ng/mL^{-1}. The authors used their method to determine the Fe(III) concentration in water samples with satisfactory results.

Transient Solvation in Ionic Liquids

As shown for previous [bmim][PF_6]+CO_2 studies [104], as well as for several other investigations discussed earlier [70, 81, 82, 136–141], time-resolved fluorescence measurements offer a versatile means by which to study the dynamics, structure, organization, and reactivity within complex systems [12, 13, 57, 145, 146]. In this regard, time-resolved fluorescence spectroscopy stands out for its superior time resolution, orthogonal information content, and ultimate sensitivity. This prospect is particularly intriguing given observations that, often, the chemistry of a species confined in a nanostructured or organized environment is drastically different from that in a bulk fluid. It is becoming increasingly apparent that ionic liquids qualify as nanostructured solvents. Additionally, they have a complicated energy landscape. Time-resolved fluorescence measurements, in general, afford information which is impossible to obtain from steady-state measurements. Investigation of solute solvation dynamics in condensed media utilizing time-resolved fluorescence is an important area of research. Many research groups have used time-resolved fluorescence to study solute solvation dynamics within various molten salts and ionic liquids. While a full discussion remains outside the scope of this review, we will introduce the concept of dipolar relaxation (Figure 13), touch on some key information accessible from this experiment, and briefly mention some work reported by various groups working in this area.

According to Ittah and Huppert [147] and Chapman and Maroncelli [148], even in high dielectric organic solvents such as propylene carbonate (PC, ε=65.1) and acetonitrile (ε=37.5), a pronounced "salt effect" on the dynamics, statistics, and energetics of dipole solvation arising from the presence of electrolyte may frequently be observed. Not only does this "ionic atmosphere" relaxation lead to an increase in the Stokes shift of excited-state dipolar probes such as coumarin 153, for example, but Ittah and Huppert also found that an increase in $LiClO_4$ concentration from 0.06 to 0.60 M in PC led to an over 6-fold decrease in relaxation time despite a 57 % overall increase in viscosity [147]. This ionic motion is basically translational and is thought to include both free ions and ion pairs, both existing in electrolyte solutions of solvents with high dielectric constant, while in the case of low dielectric solvents only ion pairs exist even at comparatively low concentration (10^{-4} M) [149]. In a series of papers that followed, Bart, Meltsin, and Huppert extended studies to organic molten

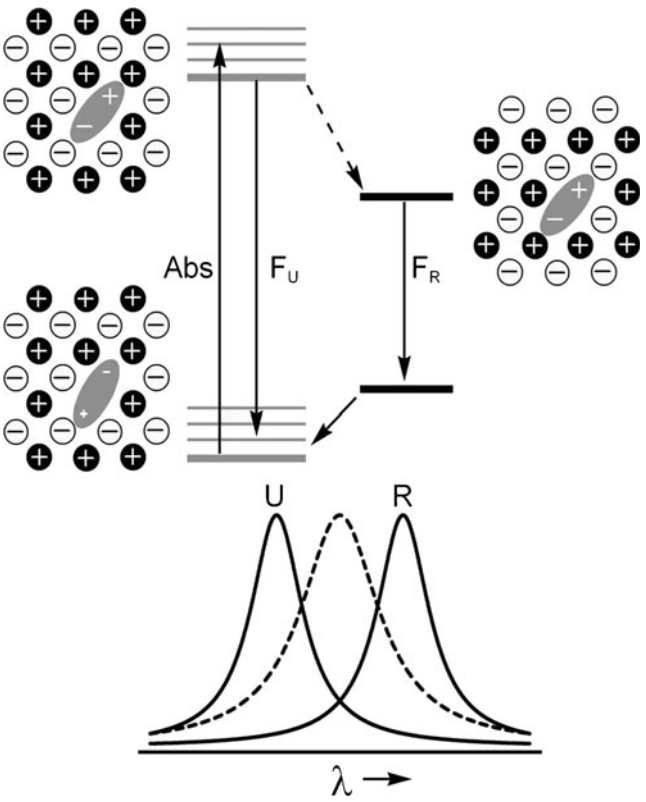

Fig. 13 Schematic representation of solvent reorganization in the vicinity of a photoexcited fluorescent probe and giving rise to spectral relaxation in an ionic liquid. U and R denote emission from unrelaxed and relaxed states, respectively

salts [47, 150–152]. It was demonstrated by measuring the Stokes shift of coumarin 153 in molten tetrabutylammonium hydrogen sulfate at 450 K using transient fluorescence that the solvation of this probe occurred on two time scales; one less than 30 ps, while the other *ca.* 300 ps [150]. In a subsequent study, these time scales were shown to depend on the cation size of the molten salt [151]; the bigger the cation, the longer the Stokes shift relaxation times. The general features of the dynamic solvation included time-dependent shifts in the fluorescence spectra that depended on the cation size of the molten salt; the average solvation time within the *same* molten salt depended on the solute [152]. Later, solvation dynamics of the same fluorescence probe coumarin 153 was studied in many different ionic liquids and ionic liquid-based systems by the research groups of Samanta [153–158], Maroncelli [159–162], Petrich [163–165], Castner [166], and Sarkar [141, 167–172]. In line with results from earlier studies on molten salts [150–152], the solvation dynamics of coumarin 153 in imidazolium ionic liquids, as characterized by the spectral shift function, were generally found to be bimodal with an ultrafast component of <5 ps, and a slow component in the ns regime with equal amplitudes [159]. That is, about 3 orders of magnitude slower than those in simple organic solvents. Interestingly, within ammonium and phosphonium ionic liquids coumarin 153 solvation indicated the absence of the ultrafast portion of the response [159, 160, 162]. In contrast with the behavior observed in imidazolium-based systems, solvation was found to occur on a single time scale. Further, the slower (i.e., ns time scale) component of the solvation dynamics in phosphonium ionic liquids was observed to be ~5-fold slower than those in imidazolium counterparts of similar viscosities [160]. Based on the results of coumarin 153 dynamic solvation within methylimidazole and butylimidazole, the rapid initial solvation was proposed to be dominated by the imidazolium moieties of the ionic liquids [164, 165].

The solvation dynamics of other fluorescence probes such as PRODAN [154–156, 173], 4-dimethylamino-4′-cyanostilbene [174, 175], 4-aminophthalimide [155–157, 176], 3,3′-diethyloxadicarbocyanine iodide [177], and Nile Red [178], in many common ionic liquids were also studied. Similar to the solvation dynamics of coumarin 153, the picosecond time-resolved fluorescence of PRODAN within [bmim][PF_6] at 298 K suggested three components with apparent relaxation times spanning over a large range of <15 ps to >10 ns to fully describe the solvent relaxation dynamics [173]. Several relaxation pathways were suggested for unquantified sub-15 ps relaxation dynamics. Between the remaining two, the faster initial component was attributed to the influence of motions of the relatively small anions, while the slower component originated in the combined influence of the cations and anions [154–156, 173]. In order to measure the complete solvation response of a probe 4-dimethylamino-4′-cyanostilbene in ionic liquids, the Maroncelli group used femtosecond Kerr-gated emission spectroscopy along with picosecond time-correlated single photon counting [174, 175]. They observed the solvation response to be widely distributed in time with contributions ranging from 100 fs to 10 ns. They were able to relate the amplitude of the faster part of the dynamics to the relative size and/or mass of the anion of the ionic liquid; the slower component was largely correlated to the viscosity of the ionic liquid. Transient solvation studies of other fluorescence probes also revealed similar outcomes; the solvation dynamics occurred in two well-separated time regimes [155–157, 176–178]. Again, the shorter of the components, in general, was assigned to the diffusional motion of the anion, whereas the longer one was attributed to the collective motion of both the ions of the ionic liquid.

These observations were further supported by the results from optically heterodyne-detected Raman-induced Kerr effect spectroscopy (OHD-RIKES) or optical heterodyne-detected optical Kerr effect (OHD-OKE) experiments [179–187]. In a series of papers, nanostructural organization and intermolecular dynamics within ionic liquids and ionic liquid mixtures using OHD-RIKES were reported by the Bartsch and Quitevis group [179–182]. Ultrafast intermolecular dynamics of some interesting ionic liquids obtained from OHD-RIKES were compared with similar and equivalent non-ionic liquid systems by Castner and coworkers [183–185]. Using OHD-OKE, the Fayer group studied orientational dynamics of supercooled ionic liquids [186] and ionic liquids at ambient temperatures [187]. Although the OHD-RIKES/OKE is a Raman-based experimental technique in general and hence detailed discussion of these observations is out of the scope of this review, they amply demonstrate the growing importance of optical measurements of dynamics in current ionic liquid research nonetheless.

During the past few years or so, the need to have ionic liquids of the highest purity to study solvation dynamics within these solvents was amply recognized by the research community involved in using fluorescence to study ionic liquid based systems. Towards this, Kobrak analyzed the solvation dynamics by modeling the time-resolved fluorescence response of coumarin 153 in two ionic liquids [bmpy]Br and [bmpy][Tf_2N] [188]. The author's results demonstrated that phenomena such as electrostatic screening operated significantly different in the two ionic liquids, and the relative importance of translational and rovibrational components of the ionic response depended significantly on the character of the ions involved. However, he suggested that the collective motion dominated the response of both ionic liquids, and that the qualitative features of this collective behavior were strikingly similar in both cases. Dynamic

solvation of the dye coumarin 153 was studied in purified phosphonium ionic liquid, hexadecyltributylphosphonium bromide, by Petrich and coworkers [189]. The ionic liquid formed micelles in water, and the bulk also existed as a liquid under the experimental conditions. The authors could compare outcomes of this system with those of an imidazolium ionic liquid, which also formed micelles in water. Analysis of the comparable situation in a phosphonium liquid was found to be not as definitive as it was proposed earlier. Specifically, in contrast, the majority of the early-time solvation was due to the organic cation. Authors pin-pointed the part of the difficulty in performing this analysis on the amount of water that was associated with the micelle. In the course of this work, the authors focused on the calculation of the solvation correlation function, C(t), and investigated how it depended upon the methods with which the "zero-time" spectrum was constructed. Kashyap and Biswas calculated the solvation dynamics in four imidazolium cation-based ionic liquids using solvation energy relaxation data in polar solvents [190]. Coumarin 153, 4-aminophthalimide, and trans-4-dimethylamino-4′-cyanostilbene were used as fluorescence probes for this purpose. The medium response to a laser-excited probe in an ionic liquid was approximated by that in an effective dipolar medium. The calculated decays of the solvent response function for these ionic liquids were found to be biphasic and the decay time constants agreed well with the available experimental and computer simulation results. Importantly, no probe dependence was found for the average solvation times in these ionic liquids. The readers at this point are referred to a review by A. Samanta on solvation dynamics in ionic liquids using dynamic fluorescence Stokes shift studies [191]. The review re-emphasizes the complexity of the solvent reorganization within ionic liquids and how it differs significantly from that in conventional polar molecular solvents. The report highlights the present understanding of the mechanism and time scale of the dynamics of solvation in ionic liquids obtained from the dynamic fluorescence Stokes shift studies on dipolar molecules.

Kimura et al. studied the fluorescence dynamics of 4′-*N*, *N*-diethylamino-3-hydroxyflavone (DEAHF) and its methoxy derivative (DEAMF) in various ionic liquids by an optical Kerr gate method [192]. DEAMF showed a single band fluorescence whose peak shifted with time by the solvation dynamics. The averaged solvation time determined by the fluorescence peak shift was found to be proportional to the viscosity of the solvent except for $[P_{14,666}][Tf_2N]$ ionic liquid. DEAHF showed dual fluorescence due to the normal and tautomer forms produced by the excited state intramolecular proton transfer (ESIPT), and the relative intensities were dependent on the time and the cation or anion of the ionic liquid. The average ESIPT time was found to be much faster than the averaged solvation time of the ionic liquids. Authors reported the ESIPT kinetics in ionic liquids to be similar to those in conventional liquid solvents such as acetonitrile. The faster ESIPT was interpreted in terms of the activation barrier-less process from the Franck-Condon state before the solvation of the normal state in the electronic excited state. The authors suggested that with the advance of the solvation in the excited state, the normal form became relatively more stable than the tautomer form making the ESIPT an activation process. Three-pulse photon echo peak shift (3PEPS) measurements were used to study the primary part (<100 ps) of the solvation dynamics in imidazolium ionic liquids with an organic dye, oxazine 4 (Ox4), used as the probe [193]. Interestingly, the ultrafast solvent response in the range of ≤300 fs exhibited dependence on the square root of the anion mass, indicating its relation to the inertial motion of anion. The inertial response of ionic liquids with chloride anions was found to be the fastest among other ionic liquids with heavier and larger anions. The authors emphasized that cationic Ox4 interacted strongly with the anion of the ionic liquid affecting the ultrafast part of the solvation by the inertial motion of anions. The authors noted that the second solvation component in the range of ≤3.5 ps had better correlation with the reduced mass and the size of both ions included, indicating the beginning of a more global solvation process.

Although we realize that it is impossible to mention all reports on solvation dynamics within ionic liquids, we would like to conclude this section by mentioning a recent article titled "Measurements of the complete solvation response of coumarin 153 in ionic liquids and the accuracy of simple dielectric continuum predictions" by Maroncelli et al. where, as implied by the title, the complete solvation response of coumarin 153 is reported over the range 10^{-13}–10^{-8} s in a variety of ionic liquids by combining femtosecond broad-band fluorescence up-conversion and picosecond time-correlated single photon counting measurements [194]. The authors used these data together with recently reported dielectric data in eight ionic liquids to test the accuracy of a simple continuum model for predicting solvation dynamics. It was found that the features of the solvation response functions predicted by the dielectric continuum model were similar to the measured dynamics of coumarin 153 in most cases. Authors pin-pointed that the predicted dynamics were observed to be systematically faster than those observed on average by a factor of 3–5. Computer simulations of a model solute/ionic liquid system were also reported to exhibit the same relationship between dielectric predictions and observed dynamics. The authors mentioned that the simulations pointed to spatial dispersion of the polarization response to be an important contributor to the over-prediction of solvation rates in ionic liquids.

Conclusions and Perspective

Fluorescence probes have proven effective in deciphering complex behavior of ionic liquids and ionic liquid-based multicomponent systems. The versatility and ease of fluorescence based methodologies, among others, are rendering them of significant use to researchers working with ionic liquids. It is increasingly clear that, due to the inherent complexity associated with ionic liquid-based systems, straightforward interpretation of fluorescence spectroscopic observables for probes dissolved in ionic liquid systems is difficult. Still, the appropriate combination of information gleaned from the responses of different fluorescence probes having varying functionality can help researchers understand the solvation within ionic liquids. This, in turn, can reveal the nature of these neoteric solvents in more depth. Powerful time-resolved fluorescence methods are finding increasing use for studying the microscopic and dynamic solvent properties of ionic liquids. It is apparent that the knowledge of the interaction/aggregate behavior of ionic liquids is a vital part of understanding how they participate as components in a mixed solvent system. In this regard, we point out the exciting prospect that water or other liquids "confined" within ionic liquid phases may be fundamentally different from the corresponding liquid in bulk. Importantly, however, the results discussed in this review demonstrate the absolute need to have ionic liquids of the highest purity (i.e., "spectroscopic-grade") for many fluorescence spectroscopy-based investigations. Clearly, further parametric studies are required to define the role of cation and anion identity in defining the properties of an ionic liquid in a systematic fashion. These challenges and others will no doubt be soon tackled by the growing ranks of ionic liquid researchers, particularly those with a bent toward spectroscopy. As already evident from ever increasing number of publications in the sub-field, computational tools have also begun to take a prominent role in understanding ionic liquids and to support outcomes of spectroscopic studies.

Acknowledgments Gary A. Baker and Sheila N. Baker would like to acknowledge the start-up funds from University of Missouri-Columbia. Siddharth Pandey would like to thank Department of Science and Technology (DST), India and Council of Scientific and Industrial Research (CSIR), India for generously funding the ongoing research on ionic liquids in his laboratory.

References

1. Reichardt C (2003) Solvents and solvent effects in organic chemistry. Wiley-VCH, Weinheim
2. Marcus Y (2002) Solvent mixtures, properties and selective solvation. Marcel Dekker, New York
3. Wasserscheid P, Welton T (2003) Ionic liquids in synthesis. Wiley-VCH, Weinheim
4. Faraday M (1849) Experimental researches in electricity I. Richard and John Taylor, London
5. Evans DF, Yamauchi A, Wei GJ, Bloomfield VA (1983) Micelle size in ethylammonium nitrate as determined by classical and quasi-elastic light scattering. J Phys Chem 87:3537–3541
6. Robinson J, Osteryoung RA (1979) An electrochemical and spectroscopic study of some aromatic hydrocarbons in the room temperature molten salt system aluminum chloride–*n*-butylpyridinium chloride. J Am Chem Soc 101:323–327
7. Wilkes JS, Levisky JA, Wilson RA, Hussey CL (1982) Dialkylimidazolium chloroaluminate melts: a new class of room-temperature ionic liquids for electrochemistry, spectroscopy, and synthesis. Inorg Chem 21:1263–1264
8. Appleby D, Hussey CL, Seddon KR, Turp JE (1986) Room-temperature ionic liquids as solvents for electronic absorption spectroscopy of halide complexes. Nature 323:614–616
9. Wilkes JS, Zaworotko MJ (1992) Air and water stable 1-ethyl-3-methylimidazolium based ionic liquids. Chem Commun 965–967.
10. Fuller J, Carlin RT, DeLong HC, Haworth D (1994) Structure of 1-ethyl-3-methylimidazolium hexafluorophosphate: model for room temperature molten salts. Chem Commun 299–300.
11. Seddon KR (1999) The international george papatheodorou symposium: proceedings. In: Dracopoulos V, Kontoyannis CG, Voyiatzis GA (eds) Boghosian S. Institute of Chemical Engineering and High Temperature Chemical Processes, Patras, pp 131–135
12. Bright FV (1995) Modern molecular fluorescence spectroscopy. Appl Spectrosc 49:14A–19A
13. Valeur B (2002) Molecular Fluorescence. Wiley-VCH, Weinheim
14. Kraayenhof R, Visser AJWG, Gerritsen HC (2002) Fluorescence spectroscopy, imaging and probes: new tools in chemical, physical and life sciences. Springer, Berlin
15. Novaki LP, El Seoud OA (1996) Solvatochromism in pure solvents: Effects of the molecular structure of the probe. Ber Bunsenges Phys Chem 100:648–655
16. Reynolds L, Gardecki JA, Frankland SJV, Horng ML, Maroncelli M (1996) Dipole solvation in nondipolar solvents: Experimental studies of reorganization energies and solvation dynamics. J Phys Chem 100:10337–10354
17. Dzyuba SV, Bartsch RA (2002) Expanding the polarity range of ionic liquids. Tetrahedron Lett 43:4657–4659
18. Earle MJ, Engel BS, Seddon KR (2004) Keto–enol tautomerism as a polarity indicator in ionic liquids. Aust J Chem 57:149–150
19. Mente SR, Maroncelli M (1999) Computer simulations of the solvatochromism of Betaine-30. J Phys Chem B 103:7704–7719
20. Znamenskiy V, Kobrak MN (2004) Molecular dynamics study of polarity in room-temperature ionic liquids. J Phys Chem B 108:1072–1079
21. Poole CF (2004) Chromatographic and spectroscopic methods for the determination of solvent properties of room temperature ionic liquids. J Chromatogr A 1037:49–82
22. Ohno H (2003) Ionic Liquids: The front and future of material developments. CMC, Tokyo
23. Rogers RD, Seddon KR (2003) Ionic liquids as green solvents: progress and prospects. ACS Symp. Ser. 856, American Chemical Society, Washington DC.
24. Rogers RD, Seddon KR,Volkov S (2002) Green industrial applications of ionic liquids. NATO Science Series, Vol. 92, Kluwer Academic Publishers, Dordrecht.
25. Rogers RD, Seddon KR (2002) Ionic Liquids: Industrial Applications for Green Chemistry. ACS Symp. Ser. 818, American Chemical Society, Washington DC.
26. Ohno H (2011) Electrochemical aspects of ionic liquids. 2nd edn. Wiley, Hobokon, New Jersey.

27. Escard MG, Seddon KR (2010) Molten salts and ionic liquids: never the twain.1st edn. Wiley, Hoboken, New Jersey.
28. Freemantle M (2009) An introduction to ionic liquids, 1st edn. RSC Publishing, Cambridge, UK
29. Malhotra S (2010) Ionic liquid applications: pharmaceuticals, therapeutics, and biotechnology (ACS Symposium Series). American Chemical Society, Maryland
30. Plechkova N, Rogers RD (2010) Seddon KR (2010) Ionic liquids: from knowledge to applications (ACS Symposium Series). American Chemical Society, Washinton DC
31. Brennecke JF, Rogers RD, Seddon KR (2007) Ionic liquids IV: not just solvents anymore (ACS Symposium Series). American Chemical Society, Washington DC
32. Kirchner B (2009) Ionic liquids (topics in current chemistry), 1st edn. Springer, New York
33. Billard I, Moutiers G, Labet A, El Azzi A, Gaillard C, Mariet C, Lützenkirchen KL (2003) Stability of divalent europium in an ionic liquid: spectroscopic investigations in 1-methyl-3-butylimidazolium hexafluorophosphate. Inorg Chem 42:1726–1733
34. Gordon CM, McLean AJ, Muldoon MJ, Dunkin IR (2003) Ionic liquids as green solvents: progress and prospects. In: Rogers RD, Seddon KR (ed) ACS Symp. Ser. 856, American Chemical Society, Washington, DC, pp 357–369.
35. Armarego WLF, Perrin DD (2003) Purification of laboratory chemicals, 5th edn. Butterworth-Heinemann, Oxford
36. Seddon KR, Stark A, Torres MJ (2000) Influence of chloride, water, and organic solvents on the physical properties of ionic liquids. Pure Appl Chem 72:2275–2287
37. Tucker SA, Amszi VL, Acree WE Jr (1992) Primary and secondary inner filtering: effect of $K_2Cr_2O_7$ on fluorescence emission intensities of quinine sulfate. J Chem Educ 69:A10–A12
38. Zagrobelny J, Bright FV (1992) In situ studies of protein conformation in supercritical fluids: trypsin in carbon dioxide. Biotechnol Prog 8:421–423
39. Flora K, Brennan JD, Baker GA, Doody MA, Bright FV (1998) Unfolding of acrylodan-labeled human serum albumin probed by steady-state and time-resolved fluorescence methods. Biophys J 75:1084–1096
40. Pandey SK, Fletcher KA, Baker SN, Baker GA (2004) Correlation between the fluorescent response of microfluidity probes and the water content and viscosity of ionic liquid and water mixtures. Analyst 129:569–573
41. Müller P (1994) Glossary of terms used in physical-organic chemistry (IUPAC recommendations 1994). Pure Appl Chem 66:1077–1184
42. Reichardt C (1994) Solvatochromic dyes as solvent polarity indicators. Chem Rev 94:2319–2358
43. Nigam S, Rutan S (2001) Principles and applications of solvatochromism. Appl Spectrosc 55:362A–370A
44. Kamlet MJ, Taft RW (1976) Solvatochromic comparison method. 1. Beta-scale of solvent hydrogen-bond (HBA) basicities. J Am Chem Soc 98:377–383
45. Taft RW, Kamlet MJ (1976) Solvatochromic comparison method. 2. Alpha-scale of solvent hydrogen-bond (HBA) acidities. J Am Chem Soc 98:2886–2894
46. Kamlet MJ, Abboud JL, Taft RW (1977) Solvatochromic comparison method. 6. π^* scale of solvent polarities. J Am Chem Soc 99:6027–6038
47. Bart E, Meltsin A, Huppert D (1994) Solvation dynamics of coumarin 153 in molten salts. J Phys Chem 98:3295–3299
48. Bonhôte P, Dias A-P, Papageorgiou N, Kalyanasundaram K, Grätzel M (1996) Hydrophobic, highly conductive ambient-temperature molten salts. Inorg Chem 35:1168–1178
49. Kalyanasundaram K, Thomas JK (1977) Solvent-dependent fluorescence of pyrene-3-carboxaldehyde and its applications in the estimation of polarity at micelle-water interfaces. J Phys Chem 81:2176–2180
50. Pandey S, Redden RA, Fletcher KA, Palmer CP (2003) Characterization of solvation environment provided by dilute poly(sulfonyl maleic anhydride-co-dodecyl vinyl ether) solutions at various pH using pyrene and 1,3-bis(1-pyrenyl)propane as fluorescence probes. Macromol Chem Phys 204:425–435
51. Baker GA, Jordan JD, Bright FV (1998) Effects of poly(ethylene glycol) doping on the behavior of pyrene, rhodamine 6 G, and acrylodan-labeled bovine serum albumin sequestered within tetramethylorthosilane-derived sol-gel-processed composites. J Sol-Gel Sci Technol 11:43–54
52. Karpovich DS, Blanchard GJ (1995) Relating the polarity-dependent fluorescence response of pyrene to vibronic coupling: achieving a fundamental understanding of the Py-polarity scale. J Phys Chem 99:3951–3958
53. Waris R, Acree WE Jr, Street KW Jr (1988) Py and BPE solvent polarity scales: effect of temperature on pyrene and benzo[ghi] perylene fluorescence spectra. Analyst 113:1465–1467
54. Dong DC, Winnik MA (1984) The Py scale of solvent polarities. Can J Chem 62:2560–2565
55. Aki SNVK, Brennecke JF, Samanta A (2001) How polar are room-temperature ionic liquids? Chem Commun 413–414.
56. Fletcher KA, Storey IA, Hendricks AE, Pandey S, Pandey S (2001) Behavior of the solvatochromic probes reichardt's dye, pyrene, dansylamide, nile red and 1-pyrenecarbaldehyde within the room-temperature ionic liquid bmimPF_6. Green Chem 3:210–215
57. Lakowicz JR (2006) Principles of Fluorescence Spectroscopy, 3rd edn. Springer, New York
58. Debye JF, Berger TA, Anderson AG (1990) Nile Red as a solvatochromic dye for measuring solvent strength in normal liquids and mixtures of normal liquids with supercritical and near critical fluids. Anal Chem 62:615–622
59. Carmichael AJ, Seddon KR (2000) Polarity study of some 1-alkyl-3-methylimidazolium ambient-temperature ionic liquids with the solvatochromic dye, Nile Red. J Phys Org Chem 13:591–595
60. Chen H, Kwait DC, Gönen ZS, Weslowski BT, Abdallah DJ, Weiss RG (2002) Phase characterization and properties of completely saturated quaternary phosphonium salts. Ordered room-temperature ionic liquids. Chem Mater 14:4063–4072
61. Paul A, Samanta A (2008) Free Volume Dependence of the Internal Rotation of a Molecular Rotor Probe in Room Temperature Ionic Liquids. J Phys Chem B 112:16626–16632
62. Nagasawa Y, Oishi A, Itoh T, Yasuda M, Muramatsu M, Ishibashi Y, Ito S, Miyasaka H (2009) Dynamic stokes shift of 9, 9′-bianthryl in ionic liquids: a temperature dependence study. J Phys Chem C 113:11868–11876
63. Santosh K, Banerjee S, Rangaraj N, Samanta A (2010) Fluorescence response of 4-(N, N′-Dimethylamino)benzonitrile in room temperature ionic liquids: observation of photobleaching under mild excitation condition and multiphoton confocal microscopic study of the fluorescence recovery dynamics. J Phys Chem B 114:1967–1974
64. Wu H, Wang H, Xue L, Shi Y, Li X (2010) Hindered intramolecular electron transfer in room-temperature ionic liquid. J Phys Chem B 114:14420–14425
65. Santosh K, Samanta A (2010) Modulation of the excited state intramolecular electron transfer reaction and dual fluorescence of crystal violet lactone in room temperature ionic liquids. J Phys Chem B 114:9195–9200
66. Zhang S, Qi X, Ma X, Lu L, Deng Y (2010) Hydroxyl ionic liquids: The differentiating effect of hydroxyl on polarity due to ionic hydrogen bonds between hydroxyl and anions. J Phys Chem B 114:3912–3920
67. Martins S, Fedorov A, Afonso CAM, Baleizao C, Berberan SMN (2010) Fluorescence of fullerene C70 in ionic liquids. Chem Phys Lett 497:43–47

68. Szmytkowski J, Bond T, Paige MF, Scott RWJ, Steer RP (2010) Spectroscopic and photophysical properties of ZnTPP in a room temperature ionic liquid. J Phys Chem A 114:11471–11476
69. Fei Z, Zhu ZR, Yang X, Meng L, Lu Q, Ang WH, Scopelliti R, Hartinger CG, Dyson PJ (2010) An internal fluorescent probe based on anthracene to evaluate cation-anion interactions in imidazolium salts. Chem Eur J 16:6473–6481
70. Liang M, Kaintz A, Baker GA, Maroncelli M (2012) Bimolecular electron transfer in ionic liquids: are reaction rates anomalously high? J Phys Chem B 116:1370–1384
71. Ben-Naim A (1989) Preferential solvation in two-component systems. J Phys Chem 93:3809–3813
72. Marcus Y (1994) Use of chemical probes for the characterization of solvent mixtures. 1. Completely nonaqueous mixtures. J Chem Soc Perkin Trans 25:1015–1021
73. Marcus Y (1994) Use of chemical probes for the characterization of solvent mixtures. 2. Aqueous mixtures. J Chem Soc Perkin Trans 28:1751–1758
74. Acree WE Jr, Wilkins DC, Tucker SA, Griffin JM, Powell JR (1994) Spectrochemical investigations of preferential solvation. 2. Compatibility of thermodynamic models versus spectrofluorometric probe methods for tautomeric solutes dissolved in binary-mixtures. J Phys Chem 98:2537–2544, and references therein
75. Fletcher KA, Pandey S (2002) Effect of water on the solvatochromic probe behavior within room-temperature ionic liquid 1-butyl-3-methylimidazolium hexafluorophosphate. Appl Spectrosc 56:266–271
76. Fletcher KA, Pandey S (2002) Solvatochromic probe behavior within binary room-temperature ionic liquid 1-butyl-3-methyl imidazolium hexafluorophosphate plus ethanol solutions. Appl Spectrosc 56:1498–1503
77. Baker SN, Baker GA, Bright FV (2002) Temperature-dependent microscopic solvent properties of 'dry' and 'wet' 1-butyl-3-methylimidazolium hexafluorophosphate: correlation with $E_T(30)$ and Kamlet–Taft polarity scales. Green Chem 4:165–169
78. Swatloski RP, Visser AE, Reichert WM, Broker GA, Farina LM, Holby JD, Rogers RD (2001). Solvation of 1-butyl-3-methylimidazolium hexafluorophosphate in aqueous ethanol – a green solution for dissolving 'hydrophobic' ionic liquids. Chem Commun 2070–2071.
79. Najdanovic VV, Esperanca JMSS, Rebelo LPN, daPointe MN, Guedes HJR, Seddon KR, Szydlowski J (2002) Phase behaviour of room temperature ionic liquid solutions: an unusually large co-solvent effect in (water plus ethanol). Phys Chem Chem Phys 4:1701–1703
80. Fletcher KA, Pandey S (2003) Solvatochromic probe behavior within ternary room-temperature ionic liquid 1-butyl-3-methyl imidazolium hexafluorophosphate plus ethanol plus water solutions. J Phys Chem B 107:13532–13539
81. Paul A, Samanta A (2008) Effect of nonpolar solvents on the solute rotation and solvation dynamics in an imidazolium ionic liquid. J Phys Chem B 112:947–953
82. Bhattacharya B, Samanta A (2008) Excited-state proton-transfer dynamics of 7-hydroxyquinoline in room temperature ionic liquids. J Phys Chem B 112:10101–10106
83. Annapureddy HVR, Hu Z, Xia J, Margulis CJ (2008) How does water affect the dynamics of the room-temperature ionic liquid 1-hexyl-3-methylimidazolium hexafluorophosphate and the fluorescence spectroscopy of coumarin-153 when dissolved in It? J Phys Chem B 112:1770–1776
84. Sarkar A, Trivedi S, Pandey S (2009) Polymer molecular weight-dependent unusual fluorescence probe behavior within 1-butyl-3-methylimidazolium hexafluorophosphate+poly(ethylene glycol). J Phys Chem B 113:7606–7614
85. Trivedi S, Pandey S (2011) Interactions within a [Ionic liquid+poly (ethylene glycol)] mixture revealed by temperature-dependent synergistic dynamic viscosity and probe-reported microviscosity. J Phys Chem B 115:7405–7416
86. Trivedi S, Malek NI, Behera K, Pandey S (2010) Temperature-dependent solvatochromic probe behavior within Ionic liquids and (ionic liquid+water) mixtures. J Phys Chem B 114:8118–8125
87. Trivedi S, Pandey S, Baker SN, Baker GA, Pandey S (2012) Pronounced hydrogen bonding giving rise to apparent probe hyperpolarity in ionic liquid mixtures with 2,2,2-trifluoroethanol. J Phys Chem B 116:1360–1369
88. Ali M, Kumar V, Pandey S (2010) Unusual fluorescein prototropism within aqueous acidic 1-butyl-3-methylimidazolium tetrafluoroborate solution. Chem Commun 46:5112–5114
89. Fletcher KA, Baker SN, Baker GA, Pandey S (2003) Probing solute and solvent interactions within binary ionic liquid mixtures. New J Chem 27:1706–1712
90. Noble D (1993) Here today, gone tomorrow. Halogenated solvents in analytical chemistry. Anal Chem 65:693A–695A
91. Via J, Taylor LT (1993) Solving process problems with supercritical fluid extraction. Chemtech 23:38–44
92. Shen TT, Schmidt CE, Card TR (1997) Assessment and control of VOC emission. Wiley & Sons, New York
93. Rafson HJ (1998) Odor and VOC control handbook. McGraw-Hill, New York
94. Johnston KP, Penninger JML (1989) Supercritical fluid science and technology. American Chemical Society, Washington DC
95. Bruno TJ, Ely JF (1991) Supercritical fluid technology: reviews in modern theory and applications. CRC Press, Boca Raton
96. Bright FV, McNally MEP (1992) Supercritical fluid technology: theoretical and applied approaches in analytical chemistry. American Chemical Society, Washington DC
97. Kiran E, Brennecke JF (1993) Supercritical Fluid Engineering Science: Fundamentals and Applications. American Chemical society, Washington DC
98. Eckert CA, Knutson BL, Debenedetti PG (1996) Supercritical fluids as solvents for chemicals and materials processing. Nature 383:313–318
99. Seddon KR (1997) Ionic liquids for clean technology. J Chem Technol Biotechnol 68:351–356
100. Hussey CL (1988) Room-temperature haloaluminate ionic liquids: novel solvents for transition metal solution chemistry. Pure Appl Chem 60:1763–1772
101. Chauvin Y, Bourbigou HO (1995) Nonaqueous ionic liquids as reaction solvents. Chemtech 25:26–30
102. Blanchard LA, Hancu D, Beckman EJ, Brennecke JF (1999) Green processing using ionic liquids and CO_2. Nature 399:28–29
103. Kazarian SG, Briscoe BJ, Welton T (2000) Combining ionic liquids and supercritical fluids: in situ ATR-IR study of CO_2 dissolved in two ionic liquids at high pressures. Chem Commun 2047–2048.
104. Baker SN, Baker GA, Kane MA, Bright FV (2001) The cybotactic region surrounding fluorescent probes dissolved in 1-butyl-3-methylimidazolium hexafluorophosphate: effects of temperature and added carbon dioxide. J Phys Chem B 105:9663–9668
105. Lu J, Liotta CL, Eckert CA (2003) Spectroscopically probing microscopic solvent properties of room-temperature ionic liquids with the addition of carbon dioxide. J Phys Chem A 107:3995–4000
106. Amotz DB, Drake JM (1988) The solute size effect in rotational diffusion experiments. A test of microscopic friction theories. J Chem Phys 89:1019–1029
107. Williams AM, Amotz DB (1992) Molecular-optical viscometer based on fluorescence depolarization. Anal Chem 64:700–703
108. Niemeyer ED, Bright FV (1998) Effects of CO_2 sorption on the rotational reorientation dynamics of a model solute dissolved in molten poly(dimethylsiloxane). Macromolecules 31:77–85

109. Kung CE, Reed JK (1989) Fluorescent molecular rotors: a new class of probes for tubulin structure and assembly. Biochemistry 28:6678–6686
110. Loutfy RO, Arnold BA (1982) Effect of viscosity and temperature on torsional relaxation of molecular rotors. J Phys Chem 86:4205–4211
111. Loutfy RO (1986) Fluorescent probes for polymer free volume. Pure Appl Chem 58:239–1248
112. Wang JS, Joanna S, Sheaff CN, Yoon B, Addleman RS, Wai CM (2009) Extraction of Uranium from aqueous solutions by using ionic liquid and supercritical carbon dioxide in conjunction. Chem Eur J 15:4458–4463
113. Kimura Y, Kobayashi A, Demizu M, Terazima M (2011) Solvation dynamics of coumarin 153 in mixtures of carbon dioxide and room temperature ionic liquids. Chem Phy Lett 513:53–58
114. Oter O, Ertekin K, Topkaya KD, Alp S (2006) Emission-based optical carbon dioxide sensing with HPTS in green chemistry reagents: room-temperature ionic liquids. Anal Bioanal Chem 386:1225–1234
115. Borisov SM, Waldhier MC, Klimant I, Wolfbeis OS (2007) Optical carbon dioxide sensors based on silicone-encapsulated room-temperature ionic liquids. Chem Mater 19:6187–6194
116. Celik S, Ertekin K, Gundogdu C, Ergun Y, Alp S (2012) Dissolved carbon dioxide sensing with phenyl-linked carbazole oxazolones in ionic liquid and ethyl cellulose moieties. Spectrosc Lett 45:74–83
117. Anderson JL, Pino V, Hagberg EC, Sheares VV, Armstrong DW (2003) Surfactant solvation effects and micelle formation in ionic liquids. Chem Commun 2444–2445.
118. Fletcher KA, Pandey S (2004) Surfactant aggregation within room-temperature ionic liquid 1-ethyl-3-methylimidazolium bis (trifluoromethylsulfonyl)imide. Langmuir 20:33–36
119. Baker GA, Pandey S (2005) Ionic liquids IIIA: fundamentals, progress, challenges, and opportunities. In: Rogers RD, Seddon KR (eds), ACS Symp. Ser. 901, American Chemical Society, Washington DC, pp 234–243.
120. Merrigan TL, Bates ED, Dorman SC, Davis JH Jr (2000) New fluorous ionic liquids act as surfactants in conventional room-temperature ionic liquids. Chem Commun 2051–2052.
121. Miskolczy Z, Sebők-Nagy K, Biczók L, Göktürk S (2004) Aggregation and micelle formation of ionic liquids in aqueous solution. Chem Phys Lett 400:296–300
122. Bowers J, Butts CP, Martin PJ, Gutierrez MCV, Heenan RK (2004) Aggregation behavior of aqueous solutions of ionic liquids. Langmuir 20:2191–2198
123. Baker GA, Pandey S, Pandey S, Baker SN (2004) A new class of cationic surfactants inspired by *N*-alkyl-*N*-methylpyrrolidinium ionic liquids. Analyst 129:890–892
124. Dattelbaum AM, Baker SN, Baker GA (2005) *N*-Alkyl-*N*-methylpyrrolidinium salts as templates for hexagonally meso-ordered silicate thin films. Chem Commun 939–941.
125. Hoffmann MM, Heitz MP, Carr JB, Tubbs JD (2003) Surfactants in green solvent systems – current and future research directions. J Disper Sci Technol 24:155–171
126. Bowlas CJ, Bruce DW, Seddon KR (1996) Liquid-crystalline ionic liquids. Chem Commun 1625–1626.
127. Firestone MA, Dzielawa JA, Zapol P, Curtiss LA, Seifert S, Dietz ML (2002) Lyotropic liquid-crystalline gel formation in a room-temperature ionic liquid. Langmuir 18:7258–7260
128. Behera K, Dahiya P, Pandey S (2007) Effect of added ionic liquid on aqueous Triton X-100 micelles. J Colloid Interface Sci 307:235–245
129. Behera K, Pandey M, Porel MD, Pandey S (2007) Unique role of hydrophilic ionic liquid in modifying properties of aqueous Triton X-100. J Chem Phys 127:184501/1–184501/10
130. Behera K, Pandey S (2007) Modulating properties of aqueous sodium dodecyl sulfate by adding hydrophobic ionic liquid. J Colloid Interface Sci 316:803–814
131. Behera K, Pandey S (2007) Concentration-dependent dual behavior of hydrophilic ionic liquid in changing properties of aqueous sodium dodecyl sulfate. J Phys Chem B 111:13307–13315
132. Behera K, Om H, Pandey S (2009) Modifying properties of aqueous cetyltrimethylammonium bromide with external additives: ionic liquid 1-hexyl-3-methylimidazolium bromide versus cosurfactant n-hexyltrimethylammonium bromide. J Phys Chem B 113:786–793
133. Behera K, Pandey S (2009) Interaction between ionic liquid and zwitterionic surfactant: A comparative study of two ionic liquids with different anions. J Colloid Interface Sci 331:196–205
134. Behera K, Pandey S (2008) Ionic liquid induced changes in the properties of aqueous zwitterionic surfactant solution. Langmuir 24:6462–6469
135. Behera K, Kumar V, Pandey S (2010) Role of the surfactant structure in the behavior of hydrophobic ionic liquids within aqueous micellar solutions. Chem Phys Chem 11:1044–1052
136. Mojumdar SS, Mondal T, Das AK, Dey S, Bhattacharyya K (2010) Ultrafast and ultraslow proton transfer of pyranine in an ionic liquid microemulsion. J Chem Phys 132:194505/1–194505/8
137. Adhikari A, Das DK, Sasmal DK, Bhattacharyya K (2009) Ultrafast FRET in a room temperature ionic liquid microemulsion: a femtosecond excitation wavelength dependence study. J Phys Chem A 113:3737–3743
138. Pramanik R, Sarkar S, Ghatak C, Rao VG, Sarkar N (2011) Solvent and rotational relaxation study in ionic liquid containing reverse micellar system: A picosecond fluorescence spectroscopy study. Chem Phys Lett 512:217–222
139. Pramanik R, Sarkar S, Ghatak C, Rao VG, Sarkar N (2011) Ionic liquid containing microemulsions: probe by conductance, dynamic light scattering, diffusion-ordered spectroscopy NMR measurements, and Study of Solvent Relaxation Dynamics. J Phys Chem B 115:2322–2330
140. Pramanik R, Sarkar S, Ghatak C, Rao VG, Setua P, Sarkar N (2010) Microemulsions with surfactant TX100, cyclohexane, and an ionic liquid investigated by conductance, DLS, FTIR Measurements, and study of solvent and rotational relaxation within this microemulsion. J Phys Chem B 114:7579–7586
141. Chakraborty A, Seth D, Chakrabarty D, Setua P, Sarkar N (2005) Dynamics of solvent and rotational relaxation of coumarin 153 in room-temperature ionic liquid 1-butyl-3-methylimidazolium hexafluorophosphate confined in Brij-35 micelles: a picosecond time-resolved fluorescence spectroscopic study. J Phys Chem A 109:11110–11116
142. Wu H, Wang H, Xue L, Li X (2010) Photoinduced electron and energy transfer from coumarin 153 to perylenetetracarboxylic diimide in bmimPF6/TX-100/water microemulsions. J Colloid Interface Sci 353:476–481
143. Wei XL, Wei ZB, Wang XW, Wang ZN, Sun DJ, Liu J, Zhao HH (2011) Phase behavior of new aqueous two-phase systems: 1-butyl-3-methylimidazolium tetrafluoroborate+anionic surfactants+water. Soft Matter 7:5200–5207
144. Zhu XS, Jiang RR (2011) Determination of iron (III) by room temperature ionic liquids/surfactant sensitized fluorescence quenching method. J Fluoresc 21:385–391
145. Bright FV, Munson CA (2003) Time-resolved fluorescence spectroscopy for illuminating complex systems. Anal Chim Acta 500:71–104
146. Bright FV, Pandey S, Baker GA (2000) Applications of lifetime measurements. In: Meyer RA (ed) Encyclopedia of Analytical Chemistry: Instrumentation and Applications. John Wiley & Sons Ltd, Chichester, pp 10447–10472

147. Ittah V, Huppert D (1990) Static and dynamic electrolyte effects on excited large dipole solvation: high dielectric constant solvents. Chem Phys Lett 173:496–502
148. Chapman CF, Maroncelli M (1991) Fluorescence studies of solvation and solvation dynamics in ionic solutions. J Phys Chem 95:9095–9114
149. Fuoss RM, Kraus CA (1933) Properties of electrolytic solutions. IV. The conductance minimum and the formation of triple ions due to the action of coulomb forces. J Am Chem Soc 55:2387–2399
150. Bart E, Meltsin A, Huppert D (1992) Static and dynamic solvation measurements of excited large dipole in molten salt. Chem Phys Lett 200:592–596
151. Bart E, Meltsin A, Huppert D (1995) Excited-state solvation dynamics in solid tetraalkylammonium salts. J Phys Chem 99:9253–9257
152. Bart E, Meltsin A, Huppert D (1994) Solvation dynamics in molten salts. J Phys Chem 98:10819–10823
153. Karmakar R, Samanta A (2002) Solvation dynamics of coumarin-153 in a room temperature ionic liquid. J Phys Chem A 106:4447–4452
154. Karmakar R, Samanta A (2002) Steady-state and time-resolved fluorescencec behavior of C-153 and PRODAN in room temperature ionic liquids. J Phys Chem A 106:6670–6675
155. Karmakar R, Samanta A (2003) Dynamics of solvation of the fluorescent state of some electron donor-acceptor molecules in room temperature ionic liquids, [BMIM][$(CF_3SO_2)_2N$] and [EMIM][$(CF_3SO_2)_2N$]. J Phys Chem A 107:7340–7346
156. Mandal PK, Samanta A (2005) Fluorescence studies in a pyrrolidinium ionic liquid: Polarity of the medium and solvation dynamics. J Phys Chem B 109:15172–15177
157. Paul A, Samanta A (2007) Solute rotation and solvation dynamics in an alcohol-functionalized room temperature ionic liquid. J Phys Chem B 111:4724–4731
158. Samanta A (2006) Dynamic Stokes shift and excitation wavelength dependent fluorescence of dipolar molecules in room temperature ionic liquids. J Phys Chem B 110:13704–13716
159. Arzhantsev S, Ito N, Heitz M, Maroncelli M (2003) Solvation dynamics of coumarin 153 in several classes of ionic liquids: Cation dependence of the ultrafast component. Chem Phys Lett 381:278–286
160. Ito N, Arzhantsev S, Heitz M, Maroncelli M (2004) Solvation dynamics and rotation of coumarin 153 in alkylphosphonium ionic liquids. J Phys Chem B 108:5771–5777
161. Ito N, Arzhantsev S, Maroncelli M (2004) The probe dependence of solvation dynamics and rotation in the ionic liquid 1-butyl-3-methylimidazolium hexafluorophosphate. Chem Phys Lett 396:83–91
162. Jin H, Baker GA, Arzhantsev S, Dong J, Maroncelli M (2004) Solvation and rotational dynamics of coumarin 153 in ionic liquids: Comparison to conventional solvents. J Phys Chem B 111:7291–7302
163. Chowdhury PK, Halder M, Sanders L, Calhoun T, Anderson JL, Armstrong DW, Song X, Petrich JW (2004) Dynamic solvation in room temperature ionic liquids. J Phys Chem B 108:10245–10255
164. Headley LS, Mukherjee P, Anderson JL, Ding RF, Halder M, Armstrong DW, Song XY, Petrich JW (2006) Dynamic solvation in imidazolium-based ionic liquids on short time scales. J Phys Chem A 110:9549–9554
165. Mukherjee P, Crank JA, Halder M, Armstrong DW, Petrich JW (2006) Assessing the roles of the constituents of ionic liquids in dynamic solvation: Comparison of an ionic liquid in micellar and bulk form. J Phys Chem A 110:10725–10730
166. Funston AM, Fadeeva TA, Wishart JF, Castner EW Jr (2007) Fluorescence probing of temperature-dependent dynamics and friction in ionic liquid local environments. J Phys Chem B 111:4963–4977
167. Chakrabarty D, Hazra P, Chakraborty A, Seth D, Sarkar N (2003) Dynamics of solvent relaxation in room temperature ionic liquids. Chem Phys Lett 381:697–704
168. Chakrabarty D, Chakraborty A, Seth D, Hazra P, Sarkar N (2004) Dynamics of solvation and rotational relaxation of coumarin 153 in 1-butyl-3-methylimidazolium hexafluorophosphate [bmim][PF_6]-water mixtures. Chem Phys Lett 397:469–474
169. Chakrabarty D, Chakraborty A, Seth D, Sarkar N (2005) Effect of water, methanol, and acetonitrile on solvent relaxation and rotational relaxation of coumarin 153 in neat 1-hexyl-3-methylimidazolium hexafluorophosphate. J Phys Chem A 109:1764–1769
170. Chakrabarty D, Seth D, Chakraborty A, Sarkar N (2005) Dynamics of solvation and rotational relaxation of coumarin 153 in ionic liquid confined nanometer-sized microemulsions. J Phys Chem B 109:5753–5758
171. Seth D, Chakraborty A, Setua P, Sarkar N (2007) Dynamics of solvent and rotational relaxation of coumarin 153 in room-temperature ionic liquid 1-butyl-3-methylimidazolium tetrafluoroborate confined in poly(oxyethylen glycol) ethers containing micelles. J Phys Chem B 111:4781–4787
172. Seth D, Chakraborty A, Setua P, Sarkar N (2007) Interaction of ionic liquid with water with variation of water content in 1-butyl-3-methylimidazolium hexafluorophosphate [bmim][PF_6]/TX-100/water ternary microemulsions monitored by solvent and rotational relaxation of coumarin 153 and coumarin 490. J Chem Phys 126: Art. No. 224512.
173. Baker SN, Baker GA, Munson CA, Chen F, Bukowski EJ, Cartwright AN, Bright FV (2003) Effects of solubilized water on the relaxation dynamics surrounding 6-propionyl-2-(N, N-dimethylamino)naphthalene dissolved in 1-butyl-3-methylimidazolium hexafluorophosphate at 298 K. Ind Eng Chem Res 42:6457–6463
174. Arzhantsev S, Jin H, Baker GA, Maroncelli M (2007) Measurements of the complete solvation response in ionic liquids. J Phys Chem B 111:4978–4989
175. Arzhantsev S, Jin H, Ito N, Maroncelli M (2006) Observing the complete solvation response of DCS in imidazolium ionic liquids, from the femtosecond to nanosecond regimes. Chem Phys Lett 417:524–529
176. Ingram JA, Moog RS, Ito N, Biswas R, Maroncelli M (2003) Solute rotation and solvation dynamics in a room-temperature ionic liquid. J Phys Chem B 107:5926–5932
177. Chakrabarty D, Chakraborty A, Hazra P, Seth D, Sarkar N (2004) Dynamics of photoisomerization and rotational relaxation of 3,3′-diethyloxadicarbocyanine iodide in room temperature ionic liquid and binary mixture of ionic liquid and water. Chem Phys Lett 397:216–221
178. Saha S, Mandal PK, Samanta A (2004) Solvation dynamics of Nile Red in a room temperature ionic liquid using streak camera. Phys Chem Chem Phys 6:3106–3110
179. Xiao D, Rajian JR, Cady A, Li SF, Bartsch RA, Quitevis EL (2007) Nanostructural organization and anion effects on the temperature dependence of the optical Kerr effect spectra of ionic liquids. J Phys Chem B 111:4669–4677
180. Xiao D, Rajian JR, Li SF, Bartsch RA, Quitevis EL (2006) Additivity in the optical Kerr effect spectra of binary ionic liquid mixtures: Implication for nanostructural organization. J Phys Chem B 110:16174–16178
181. Rajian JR, Li SF, Bartsch RA, Quitevis EL (2004) Temperature-dependence of the low-frequency spectrum of 1-pentyl-3-methylimidazolium bis(trifluoromethanesulfonyl)imide studies by optical Kerr effect spectroscopy. Chem Phys Lett 393:372–377
182. Hyun BR, Dzyuba SV, Bartsch RA, Quitevis EL (2002) Intermolecular dynamics of room-temperature ionic liquids: Femtosecond

optical Kerr effect measurements on 1-alkyl-3-methylimidazolium bis(trifluoromethylsulfonyl)imides. J Phys Chem A 106:7579–7585
183. Shirota H, Wishart JF, Castner EW Jr (2007) Intermolecular interactions and dynamics of room temperature ionic liquids that have silyl- and siloxy-substituted imidazolium cations. J Phys Chem B 111:4819–4829
184. Shirota H, Castner EW Jr (2005) Physical properties and intermolecular dynamics of an ionic liquid compared with its isoelectronic neutral binary solution. J Phys Chem A 109:9388–9392
185. Shirota H, Funston AM, Wishart JF, Castner EW Jr (2005) Ultrafast dynamics of pyrrolidinium ionic liquids. J Chem Phys 122: Art. No. 184512.
186. Li J, Wang I, Fruchey K, Fayer MD (2006) Dynamics in supercooled ionic organic liquids and mode coupling theory analysis. J Phys Chem A 110:10384–10391
187. Cang H, Li J, Fayer MD (2003) Orientational dynamics of the ionic organic liquid 1-ethyl-3-methylimidazolium nitrate. J ChemPhys 119:13017–13023
188. Kobrak MN (2007) A comparative study of solvation dynamics in room-temperature ionic liquids. J Chem Phys 127:184507/1–184507/8
189. Mukherjee P, Crank JA, Sharma PS, Wijeratne AB, Adhikary R, Bose S, Armstrong DW, Petrich JW (2008) Dynamic Solvation in Phosphonium Ionic Liquids: Comparison of bulk and micellar systems and considerations for the construction of the solvation correlation function, C(t). J Phys Chem B 112:3390–3396
190. Kashyap HK, Biswas R (2008) Dipolar solvation dynamics in room temperature ionic liquids: an Effective medium calculation using dielectric relaxation data. J Phys Chem B 112:12431–12438
191. Samanta A (2010) Solvation Dynamics in Ionic Liquids: What We Have Learned from the Dynamic Fluorescence Stokes Shift Studies. J Phys Chem Lett 1:1557–1562
192. Kimura Y, Fukuda M, Suda K, Terazima T (2010) Excited state intramolecular proton transfer reaction of 4′-N, N-diethylamino-3-hydroxyflavone and solvation dynamics. J Phys Chem B 114:11847–11858
193. Muramatsu M, Nagasawa Y, Yutaka N, Miyasaka H (2011) Ultrafast solvation dynamics in room temperature ionic liquids observed by three-pulse photon echo peak shift measurements. J Phys Chem A 115:3886–3894
194. Maroncelli M, Zhang XX, Liang M, Roy D, Ernsting NP (2012) Measurements of the complete solvation response of coumarin 153 in ionic liquids and the accuracy of simple dielectric continuum predictions. Faraday Discuss 154:409–424